The impact of different evapotranspiration models in rainfall runoff modelling using HBV-light

- a comparison of six different evapotranspiration models over three catchments in Sweden

Oscar Maxander

Division of Water Resources Engineering
Department of Building and Environmental Technology
Lund University

The impact of different evapotranspiration models in rainfall runoff modelling using HBV-light

A comparison of six different evapotranspiration models over three catchments in Sweden

By:

Oscar Maxander

Master Thesis

Division of Water Resources Engineering
Department of Building and Environmental Technology
Lund University
Box 118
221 00 Lund Sweden

Master Thesis
Division of Water Resources Engineering
Department of Building and Environmental Technology
Lund University

English title:

The impact of different evapotranspiration models in rainfall runoff modelling using HBV-light: A comparison of six different evapotranspiration models over three catchments in Sweden

Swedish title:

Paverkan av evapotranspirationsmetod vid vattenavrinningsmodellering i HBV-light: En jamførelse mellan sex olika evapotranspirationsmetoder pa tre olika avrinningsomraden i Sverige

Author:

Oscar Maxander

Supervisor:

Beatriz Quesada Montano - Hydropower Optimization Sweden, Uniper
Magnus Persson - Department of Water Resources Engineering

Examiner:

Linus Zhang - Department of Water Resources Engineering

Acknowledgements

Abstract

The choice of which potential evapotranspiration (PET) model to use when estimating streamflow using a rainfall-runoff model have been the topic of many studies. The aim with this thesis was to assess the robustness of six different PET models using HBV-light as rainfall-runoff model over three catchments in Sweden. The robustness was evaluated by using a differential split sample test (DSST) based on four climatic conditions with regard of temperature and precipitation. Data from a period of 24 years (1997-2020) was used in order to get a wide range of climatic conditions. The calibration was based on the objective function Kling-Gupta Efficiency (KGE), while the validation of the model was evaluated based on the Nash-Sutcliffe efficiency (NSE) and the volume error (VE). These objective functions are commonly used when evaluating streamflow and are know to provide good estimations of the model performance. The result showed a large difference in efficiency between each PET model and between each catchment (ranging from a KGE of 0.85-0.54 and a NSE of 0.68-0.07), proving that the optimal choice of PET model may be site specific. The Hargreaves-Samani and the Jensen-Haise model were the two PET models which showed an acceptable performance for both calibration and validation over all catchments. It could be noted that calibration and validation on similar climatic conditions would provide models with higher efficiency and that the model parameters are climate dependant.

Table of Contents

List of Figures

List of Tables

1 List of Abbreviations

2 Introduction

2.1 Background

The hydrological cycle describes the circulation of water through complex sets of processes that transfer water in different phases through the atmosphere, the land and the ocean. It consists of a set of storage's (groundwater, lakes, soil moisture and rivers) and fluxes (precipitation, evapotranspiration, infiltration and runoff) that link these storage's together [1]. The evapotranspiration is the flux which describes the combined process of evaporation from soil and water surfaces and the transpiration from plants. Approximately two-thirds of all the precipitation is returned to the atmosphere as evaporation, making it an important part of the hydrological cycle [2].

The rate of evaporation is controlled by a number of meteorological variables such as radiation, wind speed, temperature and vapor pressure deficit. Globally, most of the evaporated water comes from the oceans and other open water bodies but looking at a catchment scale most of the evaporate water comes from vegetation and land surfaces [1]. The rate of evaporation for a vegetation-covered surface doesn't only depend on meteorological variables, but also soil and plant properties and water intercepted by the vegetation surfaces (transpiration). Which of these components that is the most important depends upon local conditions [2].

Because of these complex interactions between meteorological factors and soil properties, it is very difficult to measure or estimate the actual evapotranspiration. The most important simplification has been the development of the concept of Potential Evapotranspiration (PET). It assumes that water is not limiting and is at all times sufficient to supply the requirements of the transpiring vegetation cover [2]. Empirical and semi-empirical models have been made based on the concept of PET. These models are either energy-based, temperature-based or mass transfer-based depending on their mechanisms, and vary in terms of their assumptions, data requirements, complexity and reliability [3].

When using rainfall-runoff models precipitation, temperature and the evaporative demand is needed as input, where the evaporative demand usually is introduced as the PET. Rainfall-runoff modelling is an important tool for evaluating catchment yields and responses, estimate water availability, streamflow and forecasting. It is important to have a solid model, where the parameters are carefully chosen, to achieve accurate simulations and predictions. Choosing a rainfall-runoff model is based on the purpose of answering specific questions about the hydrological process. The structure of the model can be divided into three different categories: empirical, conceptual and physical. These categories are based on how the physical processes are described in the model, varying from non-linear relationships between input and output to physical laws based on real hydrologic responses. The spatial representation of the catchment can be classified as lumped, semi-distributed or distributed depending on the needed accuracy on resolution [4]. Identifying the purpose of modeling and the availability of data is essential in order to find the model that is best suited for the intended purpose.

In this thesis a rainfall-runoff model will be used to estimate streamflow using different PET values obtained from a selection of different PET models. The rainfall-runoff model is used for operational inflow forecasting. We need a PET model that is rather simple thus does not demand too much data (given data scarcity in the Swedish mountains), and of course that gives reliable results. The question of how to represent PET in the rainfall-runoff model, to achieve the most accurate streamflow prediction, has been raised in many studies. Should a formula with large data requirements be used, with the possibility of bad spatial representation, or will a simpler formula be sufficient to achieve an acceptable accuracy? Which criteria should be used for the evaluation and how should the calibration period be chosen? These and other questions have been raised in a number of articles, in order to achieve the most accurate streamflow predictions. As previous studies have been made in climates different from Sweden this thesis will investigate these questions for the climate of northern and southern Sweden, in order to find a solid rainfall-runoff model with high accuracy on streamflow prediction. Relevant articles were reviewed to get a deeper knowledge about the subject.

2.2   Relevant literature

In a study done by (Oudin et al.[5]) they found out that simpler PET models based on extraterrestrial radiation and mean daily temperature were just as efficient as more complex formulas such as the Penman-Monteith model. The result of the study also showed that daily PET values do not generally obtain better results than mean monthly PET values in estimating streamflow using the Nash-Sutcliffe criteria. The authors compared 27 different PET models using four different lumped rainfall-runoff models over 308 catchments located in Australia, France, and the United States. By adjusting the two models which showed the best performances, the Jensen-Haise and McGuinness models, they were able to propose a simple model which only depends on radiation and temperature. This model was then evaluated and compared with the Penman-Monteith model, where the result indicated that the rainfall-runoff model efficiencies were slightly improved with this new PET model [5]. The general conclusion of the study was that there was no significant differences in the performance between the 27 PET models, indicating a lack of sensitivity of rainfall-runoff models to PET input.

Resembling results were obtained in a study done by (Bai et al.[6]).The authors found that similar streamflow results were observed when four different PET models were tested on two different rainfall-runoff models for 37 catchments with humid and non-humid climates. They found out that the reason for this was due to model parameter calibration, which eliminates the discrepancies in model inputs and generates similar runoff results. However, they found that in humid regions simulated Actual Evapotranspiration (AET) and Water Storage Capacity (WSC) were significantly different when using different PET models, although the sum of AET and WSC were similar. The main results from the study concludes that for runoff estimations, the temperature-based models can yield high model performance in both humid and non-humid regions [6].

In a study done by (Dakhlaoui et al.[7]) it could be concluded that in semi-arid regions, discharge simulations are not sensitive to PET estimates since AET is mainly controlled by the availability of soil moisture. By using a temperature-based PET model, they investigate the sensitivity of discharge projections for different Representative Concentration Pathway (RCP) scenarios based on the Nash-Sutcliffe Efficiency (NSE) and relative volume error. A RCP describe different climate futures, depending on the volume of greenhouse gases emitted. The projected discharge for the different RCP scenarios was slightly lower when using mean values compared to daily. But the difference in volume change did not exceed 9 % for both periods and the considered RCP scenarios [7]. A similar study was done by (Ali et al.[8]). They concluded that temperature and precipitation were the most sensitive parameters to streamflow.

In another study done by (Weiß and Menzel[9]) the obtained result showed that radiation-based PET models provided the highest accuracy on streamflow predictions when used on a global scale. This was mostly due to the simplicity of the model as the more complex PET models showed a higher sensitivity in data measurement errors. Similar results were obtained in a study done by (Seong et al.[10]). The effect on projected streamflow under changing climatic conditions was evaluated for five PET models for a basin in the northeastern United States. They concluded that the selection of PET model were important in order to achieve accurate streamflow predictions. Hamon and Thornthwaite were the two PET models which showed acceptable results compared to the more complex PET models such as Penman-Monteith, where poor streamflow predictions could be observed.

Several different studies have searched for the data length and hydrological conditions which results in the most reliable calibration and predictions for a lumped conceptual model. One problem is that the model usually is needed for estimation under conditions different from those applied under model development and calibration. A study done by (Motavita et al.[11]) showed that hydrological conditions had a stronger impact than time-series length for calibration on their specific catchment. By using a Differential Split-Sample Test (DSST), that is, by dividing the time-period into wet, mixed or dry periods, and using different length on calibration and validation periods, they were able to test the agility and robustness of the model. A higher efficiency was obtained when calibrating on dry conditions, and using a time-series of 8 years or longer led to overconfident predictions. However, parameter uncertainty caused considerably different predictions although the best-suited parameters were used. Similar results were obtained in study done by Dakhlaoui et al.[12]. By using a DSST dividing the time-period into sub-periods based on temperature and precipitation, they found that the models showed a higher efficiency when validated on colder and wetter periods. Some set of parameters achieved very good estimations while others produced poor estimations for future conditions, proving that there is a climate dependence of the model parameters. This problem has been observed in many other studies where the DSST have been used (Seibert[13], Dakhlaoui et al.[14])).

2.3 Aims and objectives

The aim of this study was to explore the impact of different PET models on predictions of stream flow using a lumped rainfall-runoff model in three catchments in Sweden. This was done by 1) comparing the accuracy of streamflow prediction, based on selected objective functions, for six different PET models, 2) assessing the performance of the different PET models for catchments with varying meteorological and hydrological conditions, exploring their robustness efficiency for different calibration periods, 3) evaluate the climate dependence of the model parameters by using a DSST.

2.4 Methodology

Six different PET models were considered in this study: three temperature-based, two radiation-based and one that uses a combination of both temperature and radiation. The Swedish Meteorological and Hydrological Institutes (SMHI) weather stations in and around the catchments were used to obtain the required meteorological data for each PET model. Both daily values and mean annual values were calculated for each PET model. Their performance were evaluated over three catchments, each with an active hydro-power station, located in the south and north of Sweden. For two of the catchments, both located in the north, current values used for estimating PET were given by the Hydro-power company (Uniper). These values were also used to see how well they estimate streamflow. Discharge values were obtained by Uniper for two of the catchment and by SMHI for the third catchment. The conceptual rainfall-runoff model HBV-light (Seibert[13]) was used in its lumped set-up for this study. The model is based on the HBV Model software developed by S.Bergström at SMHI. A conceptual model was chosen as it is defined by a simple model structure which makes it easy to calibrate [4].

The DSST were used for calibration and validation for each PET model. It is a way to divide the reference period into distinct hydrological years with varying climatic conditions. By doing so it is possible to study the effects of chosen calibration and validation period on parameter performance of the model. This is commonly used to provide operational forecasts for the hydro power industry in Sweden. The calibrated rainfall-runoff model will be evaluated on how well it performs over a more diverse climate and it will be easier to identify robust model parameters (Motavita et al.[11]). This have been proved to work well in previous studies, e.g. in Dakhlaoui et al., where different climatic conditions have been used.

The reference period were divided into four sub-periods. Each PET model was calibrated on each sub-period and then validated over the rest. For calibration an built-in calibration function called Monte-Carlo was used. By using an objective function when calibrating the model, the Monte-Carlo function creates random sets of parameters in order to increase the accuracy of the model predictions, taking into account the parameter uncertainty. 50 000 parameter sets were randomly sampled were the Kling-Grupta Efficiency (KGE) was

chosen as objective function for calibration. The 100 parameter sets with the highest KGE value were then saved and used for validation. During validation the model performance was evaluated with regard of the NSE and the Volume Error (VE). A comparison was then made between the accuracy of each PET model, sub-period and catchment.

3   PET models

Three temperature-based, two radiation-based and one combined PET model were compared and evaluated. These models were chosen based on required input data and their efficiency from similar studies.

3.1   Temperature-based models

3.1.1   Thornthwaite model

The Thornthwaite equation is a simple model used for estimating monthly potential evapotranspiration. It uses the mean monthly temperature as only input parameter. The obtained values is then adjusted according to length of the month and the theoretical sunshine hours for the latitude of interest [15]. The equation is given by:

$$PET_{TH} = \frac{N}{12} \cdot \frac{d}{30} \cdot 16 \left(\frac{10 \cdot T}{I}\right)^{\alpha} \quad (mm/month) \tag{1}$$

N = mean daily daylight hours for each month (h)
d = days of the month (d)
T = mean monthly temperature (°C)
I = annual heat index (°C)

The Annual Heat Index I is calculated as the sum of the Monthly Heat Indices:

$$I = \sum_{t=1}^{12} i \tag{2}$$

Where:

$$i = \left(\frac{T}{5}\right)^{1.514} \tag{3}$$

i = monthly thornthwaite heat index (°C)

The constant α is calculated according to the equation:

$$\alpha = 675 \cdot 10^{-9} \cdot I^3 - 771 \cdot 10^{-7} \cdot I^2 + 1792 \cdot 10^{-5} \cdot I + 0.49239 \qquad (4)$$

The Thornthwaite equation is developed from water balance studies carried out in the eastern/central USA. To get daily PET values the obtained monthly values were divided with the length of each month.

3.1.2 Hargreaves-Samani model

The Hargreaves-Samani equation is the most commonly used temperature-based model for estimating PET. It uses the daily maximum, minimum and mean temperature as input parameters [16]. The Hargreaves model was originally calibrated for semi-arid regions of California but have been used in several other studies with different climate [5], [6], [7].

$$PET_{HS} = 0.023\sqrt{T_{max} - T_{min}} \cdot (T_{mean} + 17.8) \cdot R_\alpha \quad (mm/day) \qquad (5)$$

R_α = extraterrestrial radiation ($MJm^{-2}day^{-1}$)

This equation is known to overestimate the PET in conditions of high relative humidity and underestimate under wind conditions where $u > 3$ m/s [17].

3.1.3 Linacre model

The Linacre equation requires latitude and height for the measurement point, daily mean temperature and daily dew-point temperature. The equation is not suitable for hourly prediction but works well for longer intervals [18].

$$PET_{LIN} = \frac{\frac{500 \cdot (T_{mean} + 0.006 \cdot h)}{100 - Lat} + 15(T_{mean} - T_{dew})}{80 - T_{mean}} \quad (mm/day) \qquad (6)$$

h = height of measurement station (m)
Lat = latitude of measurement station

3.2   Radiation-based models

3.2.1   Jensen-Haise model

The Jensen-Haise equation requires daily mean temperature and solar radiation as input for calculating the PET [5].

$$PET_{JH} = \frac{R_a}{\lambda} \cdot \frac{T_{mean}}{40} \quad (mm/day) \tag{7}$$

λ = latent heat of vaporization (2.45 $MJkg^{-1}$)
R_α = extraterrestrial radiation ($MJm^{-2}day^{-1}$)

3.2.2   McGuinness model

The McGuinness equation is a variation of the Jensen-Haise equation. It also requires daily mean temperature and solar radiation as input for calculating the PET [5].

$$PET_{MG} = \frac{R_a}{\lambda} \cdot \frac{T_{mean} + 5}{68} \quad (mm/day) \tag{8}$$

λ = latent heat of vaporization (2.45 $MJkg^{-1}$)
R_α = extraterrestrial radiation ($MJm^{-2}day^{-1}$)

3.3   The FAO Penman-Monteith model

The FAO Penman-Monteith equation is recommended by the Food and Agriculture Organization of the United Nations (FAO) and World Meteorological Organization as a standard model to calculate PET_o [18]. It requires radiation, daily mean temperature, humidity data and wind speed data as input. The equation determines the evapotranspiration from the hypothetical grass reference surface as [17]:

$$PET_{PM} = \frac{0.408\triangle(R_n - G) + \gamma\frac{900}{T_{mean}+273}u_2(e_s - e_a)}{\triangle + \gamma(1 + 0.34u_2)} \quad (mm/day) \tag{9}$$

R_n = net radiation at the crop surface ($MJm^{-2}day^{-1}$)
G = soil heat flux density ($MJm^{-2}day^{-1}$)
T_{mean} = mean air temperature at 2 m height ($°C$)
U_2 = wind speed at 2 m height ($ms-1$)

e_s = saturation vapour pressure (kPa)
e_a = actual vapour pressure (kPa)
$\triangle$ = slope vapour pressure curve $(kPa°C^{-1})$
γ = psychometric constant $(kPa°C^{-1})$

The main problem with this formula lies in the difficulty of obtaining adequate measurement of the vegetation factors, and especially of R_s (surface resistance). In cases where the vegetation canopies are not homogeneous this one-dimensional approximation may lead to significant errors [2]. As the model require a lot of data it is also sensitive to measurement errors.

4 Study area

Three catchments in Sweden were used for the evaluation of the different PET models. The catchments were chosen so that they would represent areas with different latitude, topography and climate. The following section describes each catchment and the meteorological stations used for data input. For each map all the weather stations used to collect meteorological data are represented as black triangles. The red dot represents the location where the data for observed streamflow is obtained. Figure 1 shows an overview of the location of the catchments. All catchment areas are obtained from SMHI.

Figure 1: Overview of the catchments

4.1 Borgasjön

4.1.1 Geography

Borgasjön is a lake situated in the north of Sweden. It has an area of 30.5 km^2 and is located at a mean of 469 m above sea level. The catchment for Borgasjön extends from Lat. 65°05′ to 64°80′ and Lon. 14°25′ to 15°04′, covering an area of 514 km^2 [Figure 2]. It mostly consists of forested area (about 50%) and tundra (about 27%). The elevation within the catchment ranges from 467 m to 1 130 m above sea level.

4.1.2 Meteorology

The warmest months are June, July and August with an average maximum temperature of 18 °C in July. Winter extends from November to March with an average maximum temperature of -11 °C in January. Average annual temperature is maximum 3 °C and minimum -5 °C. On average July is the wettest month and March the driest. Average annual precipitation is 409 mm [19]

4.1.3 Data collection

Weather stations used for the collection of meteorological data is presented in Table 1. Due to data limitation some stations could only be used for precipitation data. Data for observed runoff were obtained by Uniper and is filtered with a Gaussian filter. The areal precipitation for the catchment was calculated using the Thiessen polygon method. Daily data between $1997/01/01 - 2019/12/31$ were used for Borgasjön.

Name	Location	Elevation	Data	Areal Weight
Ankarvattnet D	64.8779, 14.2293	460	P	0.45
Avasjö-B.fjäll D	64.8340, 15.0748	535	P	0.45
Gielas A	65.3269, 15.0645	578	P, T, u, T_{dew}	0.10
Stekenjokk	65.0929, 14.5055	1037	T, u, T_{dew}	
Östersund	63.1970, 14.4798	372	$Sunshine\ hours$	

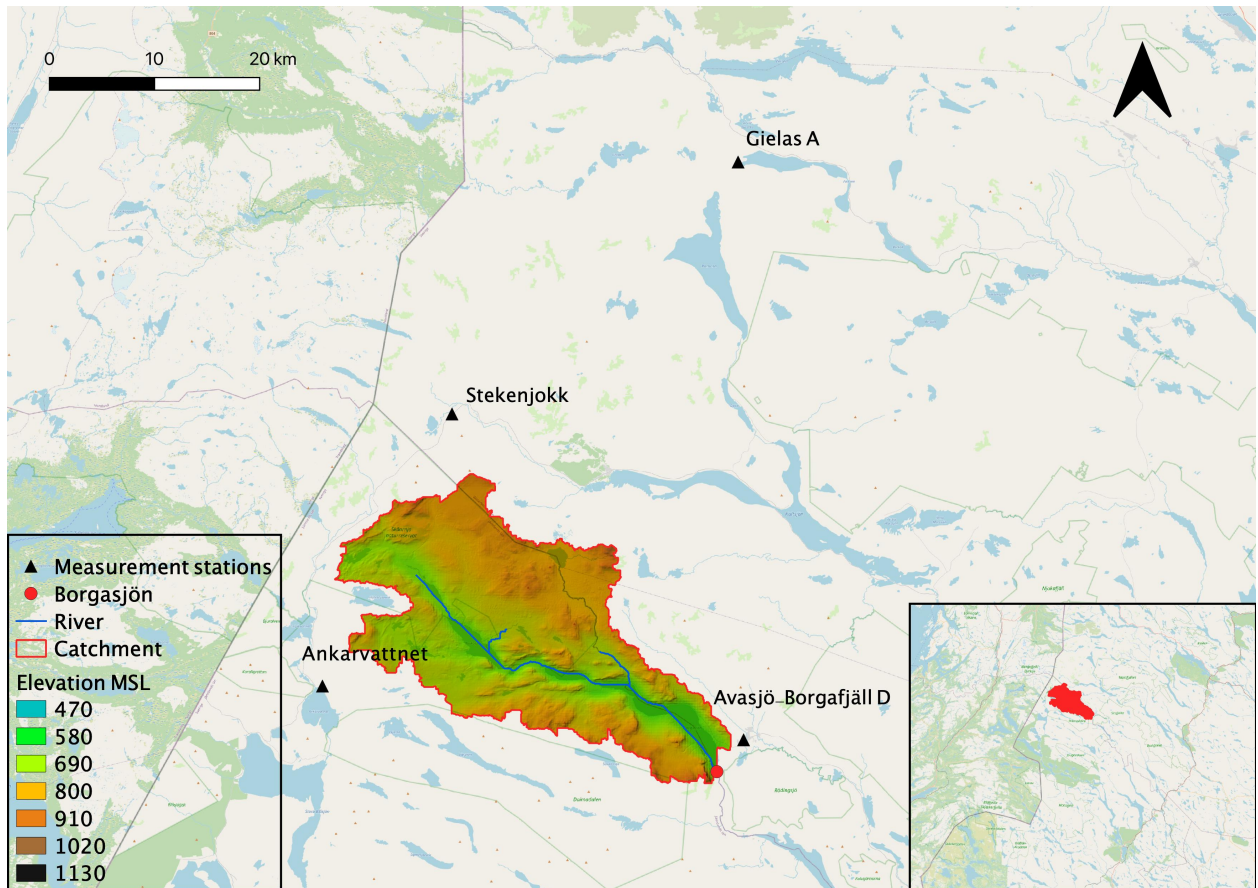Table 1: Measurement stations Borgasjön

Figure 2: Catchment Borgasjön

4.2 Lännässjön

4.2.1 Geography

Lännässjön is a lake situated in the middle of Sweden. It has an area of 19.3 km^2 and is located at a mean of 437 m above sea level. The catchment for Lännässjön extends from Lat. 62°55′ to 63°04′ and Lon. 12°46′ to 14°11′, covering an area of 1 194 km^2 [Figure 3]. It mostly consists of forested area (about 69%). The elevation within the catchment ranges from 440 m to 1386 m above sea level. The catchment is a part of the Ljungan basin which ends in Bottenhavet in the Baltic sea.

4.2.2 Meteorology

The warmest months are June, July and August with an average maximum temperature of 19 °C in July. Winter extends from December to March with an average maximum temperature of -6 °C in January. Average annual temperature is maximum 6 °C and minimum -3 °C. On average July is the wettest month and February the driest. Average annual precipitation is 557 mm [19].

4.2.3 Data collection

Weather stations used for the collection of meteorological data is presented in Table 2. Due to data limitation some stations could only be used for precipitation data. The stations is controlled by SMHI and the data is fetched from their website. Data for observed runoff were obtained by Uniper. The runoff data is filtered with a Gaussian filter to reduce the noise in the observed values, which is caused by the regulation of the flow.

The areal precipitation for the catchment was calculated using the Thiessen polygon method. Each station was given a weight based on its relative area in the catchment and the areal precipitation could be calculated by summarizing the corrected precipitation for each station. Daily data between $2001/01/01 - 2020/12/31$ were used for Lännässjön.

Name	Location	Elevation	Data	Areal Weight
Börtnan A	62.7548, 13.8427	467	P, T, u, T_{dew}	0.5
Höglekardalen	63.0785, 13.7488	595	P	0.09
Klövsjöhöjden A	62.4952, 14.1542	803	P, T, u, T_{dew}	0.01
Ljusnedal	62.5493, 12.6043	585	P	0.17
Vallbo	63.1557, 13.0697	581	P	0.22
Östersund	63.1970, 14.4798	372	*Sunshine hours*	

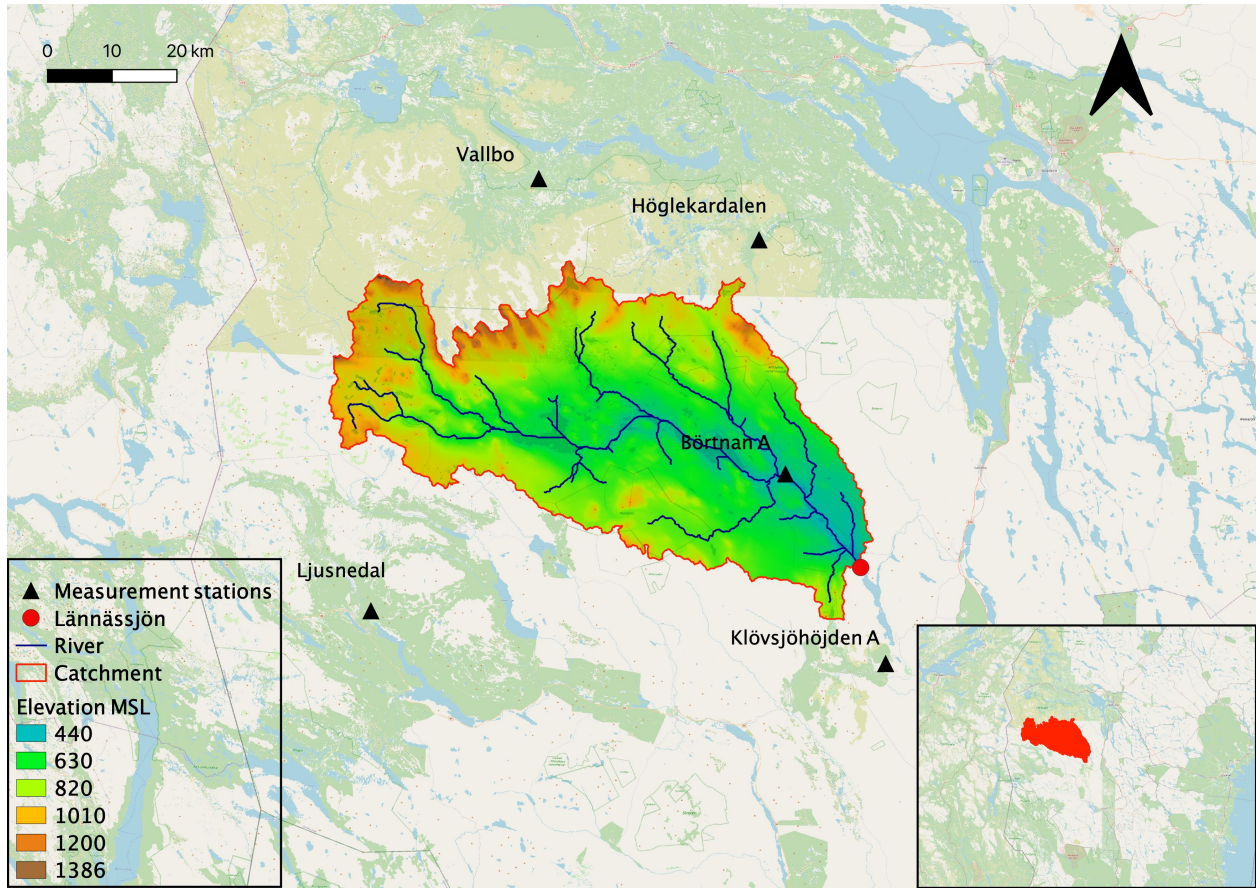Table 2: Measurement stations Lännässjön

Figure 3: Catchment Lännässjön

4.3 Yngeredsforsen

4.3.1 Geography

Yngeredsforsen is located in the river Ätran, which is a river situated in the south of Sweden. It is about 240 km long, reaching from Gullered in Västragötaland to Falkenberg in Halland. Yngeredsforsen is located at (Lat. 57°03′, Lon. 12°76′) with an catchment upstream covering 2 574 km^2 [Figure 4]. The catchment mostly consists of forested area and the elevation ranges from 65 m to 327 m above sea level.

4.3.2 Meteorology

The warmest months are June, July and August with an average maximum temperature of 22 °C in July. Winter extends from December to March with an average maximum temperature of 3 °C in January. Average annual temperature is maximum 12.1 °C and minimum 6.3 °C. On average July is the wettest month and April the driest. Average annual precipitation is 603 mm [19].

4.3.3 Data collection

Weather stations used for the collection of meteorological data is presented in Table 3. Due to data limitation some stations could only be used for precipitation data. Data for observed runoff were obtained by SMHI. The areal precipitation for the catchment was calculated using the Thiessen polygon method. Daily data between $1997/01/01 - 2019/12/31$ were used for Yngeredsforsen.

Name	Location	Elevation	Data	Areal Weight
Hid D	57.3658, 13.0486	140	P	0.38
Sjötofta D	57.3848, 13.2974	170	P	0.27
Skeppshult D	57.1210, 13.4028	160	P	0.05
Torup A	56.9494, 13.0601	132	P, T, u, T_{dew}	0.03
Ullared	57.1134, 12.7732	122	P, T, u, T_{dew}	0.27
Växjö	56.9269, 14.7305	182	$Sunshine\ hours$	

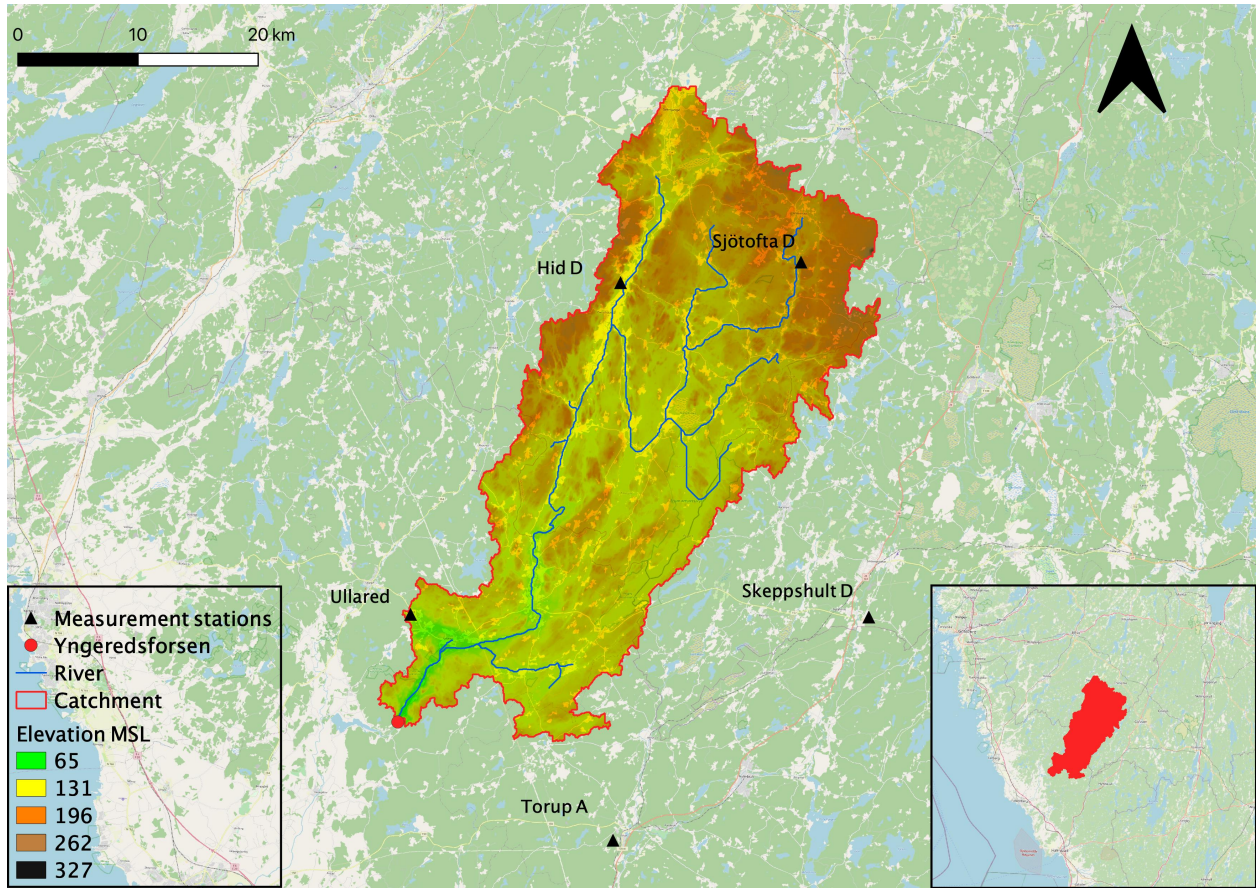Table 3: Measurement stations Yngeredsforsen

Figure 4: Catchment Yngeredsforsen

5 Rainfall-runoff model

5.1 HBV-light

HBV-light is a hydrological runoff model based on the HBV model developed by SMHI 1972 (Bergström[20]). It is a lumped/semi-distributed model, which means that hydrological processes are lumped together in defined zones over the catchment. These zones are based on vegetation characteristics and elevation. The model continuously simulates fluxes of water within the catchment. The model can be used to calculate river discharge by using precipitation, temperature and evapotranspiration as input. Observed river flows are needed to calibrate the model and the accuracy of the model increases with increasing length of the data series. The model consists of different routines which describes the hydrological process in order to estimate streamflow within the catchment.

5.1.1 Snow routine

The model defines precipitation as snow if the temperature is below the threshold temperature, T_t. If the temperature then goes above the threshold temperature, the snow starts to melt. The melt rate is defined by the degree-day method:

$$M = C_{fmax}(T - T_t) \tag{10}$$

Where C_{fmax} is typically around 4 mm $d^{-1}C^{-1}$.

The snow retains melt water until it exceeds a certain portion of the water equivalent of the snow pack. This portion is usually 10 percent of the water equivalent and must be exceeded before the snow melt can be calculated as runoff. If the temperature decreases below the threshold temperature again the water can refreeze according to:

$$R = C_{fr}C_{fmax}(T_t - T) \tag{11}$$

Where C_{fr} is usually around 0.05. This means that the refreezing is twenty times less efficient than the melting. All precipitation which is simulated as snow is multiplied by a correction factor Sf_{cf}.

5.1.2 Soil routine

Water from precipitation and snow melt will fill the soil box and contribute to the groundwater recharge depending on the relation between water content of the soil box SM and its

largest value FC. This relation is defined as:

$$\frac{Recharge}{P} = (\frac{SM}{FC})^{\beta} \tag{12}$$

Where β range between zero and one.

Actual evaporation from the soil box equals the potential evaporation if SM/FC is above LP, while a linear reduction is used when SM/FC is below LP. This is defined by the equation:

$$E_{act} = E_{pot} min(\frac{SM}{FC * LP}, 1) \tag{13}$$

5.1.3 Groundwater routine

In the HBV-light model the groundwater is represented by two boxes. The lower box SLZ represents the slowly reacting flow which feeds into the base flow. The upper box SUZ represents the upper groundwater which reacts quicker to precipitation and snow melt. $PERC$ defines the maximum rate of flow from the upper box to the lower. The runoff is represented as a combination of three groundwater flows: Q_0, Q_1, Q_2. All these flows are linear and dependant on the water level in the box, but the combined runoff will be non-linear.

$$Q_{GW}(t) = K_2 SLZ + K_1 SUZ + K_0 max(SUZ - UZL, 0) \tag{14}$$

5.1.4 Routing routine

The runoff is finally transformed by a triangular weighting function defined by the parameter MAXBAS to give the simulated runoff. This is defined as:

$$Q_{sim}(t) = \sum_{i=1}^{MAXBAS} c(i)Q_{GW}(t - i + 1) \tag{15}$$

where

$$c(i) = \int_{i}^{i-1} \frac{2}{MAXBAS} - |u - \frac{MAXBAS}{2}| \frac{4}{MAXBAS^2} du \tag{16}$$
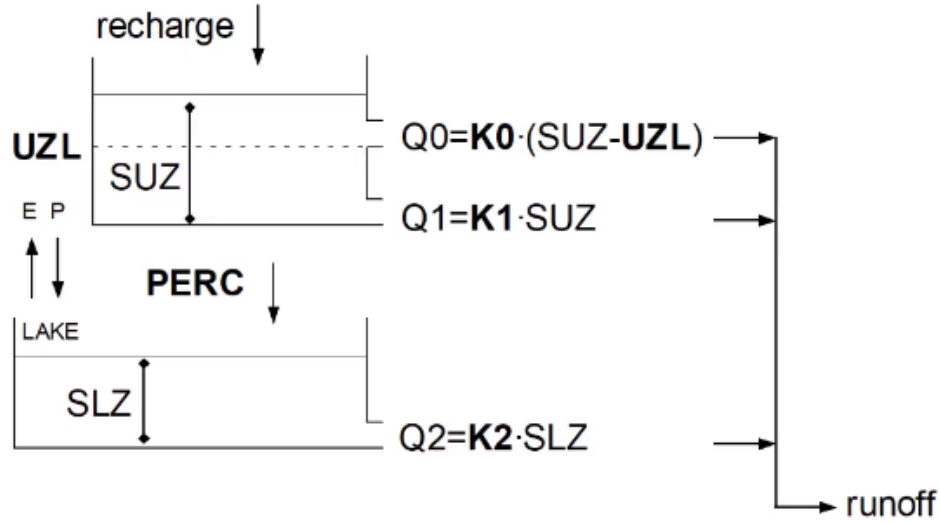
Figure 5: Groundwater routine

5.1.5 Parameters

There is a number of parameters which describes the different processes during the different routines. The parameters have to be calibrated in order to achieve a model with streamflow predictions of high efficiency. The parameters used in HBV-light is presented in Table 2

5.2 Objective functions

For calibration of the model parameters the KGE were chosen as objective function. It has been used as objective function in similar studies where the DSST was applied, and has been proved to generate robust parameters [12], [11]. For validation the model performance were evaluated based on the NSE and the VE. These objective functions are commonly used when evaluating simulated streamflow using rainfall-runoff models. The objective functions are described more thoroughly in the following section.

5.2.1 Kling-Gupta efficiency

The Kling-Gupta efficiency (KGE) is an improvement of the Nash-Sutcliffe efficiency. It considers the error in the mean, the variability and the dynamics. By using multiple objectives for model calibration it reduce the risk for overfitting of model parameters. It is based on

Parameter	Subroutine	Description	Unit	Range
TT	Snow	Threshold temperature	°C	[-inf, inf]
$CFMAX$	...	Degree-day factor	$mm°C^{-1}d^{-1}$	[0, inf]
SP	...	Seasonal variability	-	[0, 1]
$SFCF$	...	Snowfall correction factor	-	[0, inf]
CFR	...	Refreezing coefficient	-	[0, inf]
CWH	...	Water holding capacity	-	[0, inf]
FC	Soil moisture routine	Maximum soil moisture storage	mm	[0, inf]
LP	...	SM above which AET reaches PET	-	[0, 1]
$BETA$	...	Relative cont. to runoff from rain or snowmelt	-	[0, inf]
$PERC$	Response routine	Threshold parameter	mm/dt	[0, inf]
UZL	...	Threshold parameter	mm	[0, inf]
$K0$	...	Storage coefficient 0	$1/dt$	[0, 1]
$K1$	...	Storage coefficient 1	$1/dt$	[0, 1]
$K2$	...	Storage coefficient 2	$1/dt$	[0, 1]
$MAXBAS$	...	Triangular weighting function	dt	[1, 100]

Table 4: Parameters HBV-light

the assumptions of data linearity and data normality [21]. The equation is given as:

$$KGE = 1 - \sqrt{(r-1)^2 + (\frac{\sigma_{sim}}{\sigma_{obs}} - 1)^2 + (\frac{\mu_{sim}}{\mu_{obs}} - 1)^2} \tag{17}$$

where r is the linear correlation between observations and simulation, $\frac{\sigma_{sim}}{\sigma_{obs}}$ is a measure of the flow variability error and $\frac{\mu_{sim}}{\mu_{obs}}$ is a bias term.

$KGE = 1$ indicates a perfect fit between observed and simulated values while $KGE < 0$ indicates that the mean of observations provides better estimates than simulations [21].

5.2.2 Nash–Sutcliffe model efficiency

The Nash–Sutcliffe model efficiency (NSE) is used to assess the predictive skill of hydrological models. It is based on the ration between simulated and observed values where $NSE = 1$ equals a perfect fit. Values below zero is equal to a poor efficiency where observed mean is

a better predictor than the model. The equations is give by:

$$NSE = 1 - \frac{\sum_{t=1}^{T}((Q_m)^t - (Q_o)^t)^2}{\sum_{t=1}^{T}((Q_o)^t - (Q_{mo})^t)^2} \tag{18}$$

where Q_m is the simulated discharge, Q_o is the observed discharge and Q_{mo} is the mean of observed discharge.

5.2.3 Volume error

The Volume Error (VE) represents the agreement of cumulative runoff volume during the simulation period and is expressed through the proportional difference to observed values [14]. The optimal value is one.

$$VE = 1 - (\sum_{t=1}^{T} Q_{obs} - \sum_{t=1}^{T} Q_{sim}) / \sum_{t=1}^{T} Q_{obs} \tag{19}$$

6 Simulation

6.1 Calibration and validation

For each catchment the reference period, the period for which the data is obtained, was divided into four climatic conditions: Hot/Dry (HD), Hot/Wet (HW), Cold/Dry (CD) and Cold/Wet (CW). The annual temperature for each year is calculated as the average daily temperature for that year. The annual precipitation for each year is calculated as the sum of the precipitation for that year. Years with an annual temperature above the average were classified as hot years, and below the average as cold years. Likewise, years with an annual precipitation above the average were classified as wet, and below as dry. Previous studies [11], [12], [14] showed that 3-8 years were considered sufficient for each sub-period for calibration using a DSST. The years within each sub-period do not have to be continuous.

Each PET model will be calibrated for each catchment and sub-period. This will result in 72 models that will be simulated in the HBV-light software. For each PET model, 50 000 parameter sets were randomly sampled from a uniform probability distribution with ranges shown in Table 8. This is a function called Monte-Carlo simulation and it will generate optimized parameter sets based on selected objective function. 50 000 parameter sets were used due to the time limit of the thesis. The rainfall-runoff model was then validated using the 100 sampled parameter sets with the highest KGE value for each PET model, sub-period and catchment. During validation the model performance was evaluated with regard of the

NSE and VE. Each PET model were validated over all sub-periods and the whole reference period. Figure 6 shows an overview of the workflow for model calibration and validation.
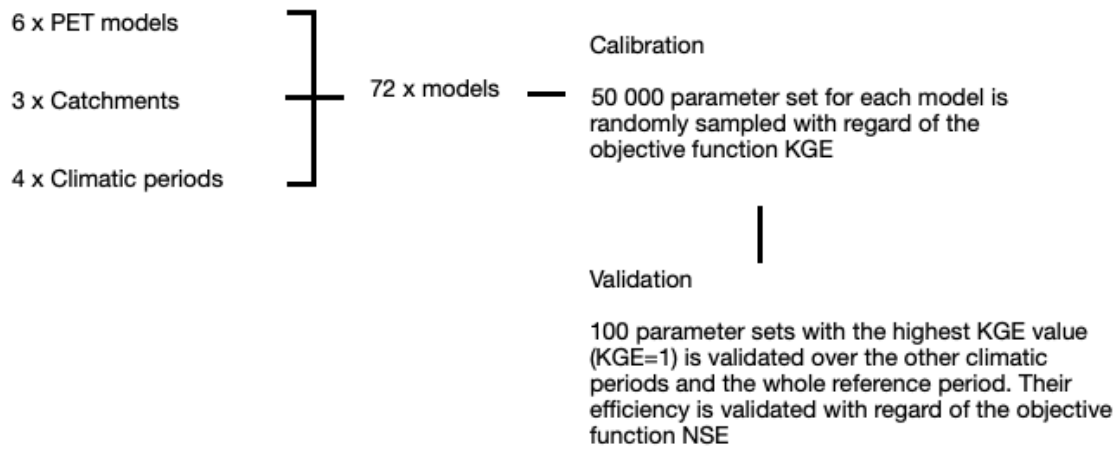

Figure 6: Chart over the work flow for calibration and validation of each model

6.1.1 Sub-periods

For Borgasjön 6 HD-, 6 HW-, 7 CD- and 4 CW-years were obtained. Figure 7 shows the annual precipitation and average annual temperature for each year. The average annual precipitation and temperature for the whole reference period were 882 mm respectively $-0.7°C$ and is represented as the black lines in the figure. The difference in average precipitation and temperature range from -14% to $+14\%$ and from $-0.7°C$ to $+0.6°C$ between the different sub-periods. The corresponding sub-period for each year is presented in Table 5.

Sub-period	Year
Hot/Dry	2002, 2006, 2007, 2008, 2014, 2016
Hot/Wet	2000, 2003, 2005, 2011, 2013, 2015
Cold/Dry	1997, 1999, 2009, 2010, 2012, 2018, 2019
Cold/Wet	1998, 2001, 2004, 2017

Table 5: Sub-periods Borgasjön

For Lännässjön 6 HD-, 6 HW-, 4 CD- and 4 CW-years were obtained. Figure 8 shows the annual precipitation and average annual temperature for each year. The average precipitation and temperature for the whole reference period were 568 mm respectively $1.8°C$ and is represented as the black lines in the figure. The difference in average precipitation and temperature range from -9% to $+12\%$ and from $-1.3°C$ to $+0.6°C$ between the different sub-periods. The corresponding sub-period for each year is presented in Table 6.

Sub-period	Year
Hot/Dry	2003, 2007, 2008, 2016, 2018, 2020
Hot/Wet	2005, 2006, 2011, 2014, 2015, 2019
Cold/Dry	2002, 2004, 2013, 2017
Cold/Wet	2001, 2009, 2010, 2012

Table 6: Sub-periods Lännässjön

For Yngeredsforsen 3 HD-, 9 HW-, 7 CD- and 4 CW-years were obtained. Figure 9 shows the annual precipitation and the average annual temperature for each year. The average precipitation and temperature for the whole reference period were 1122 mm respectively $7.2°C$ and is respresented as the black lines in the figure. The difference in average precipitation and temperature range from -19% to $+15\%$ and from $-0.7°C$ to $+0.6°C$ between the different sub-periods. The corresponding sub-period for each year is presented in Table 7.

This proves that there is a substantial climatic difference between each sub-period, which will provide an important contrast between calibration and validation.

Sub-period	Year
Hot/Dry	2002, 2016, 2018
Hot/Wet	2000, 2006, 2007, 2008, 2011, 2014, 2015, 2017, 2019
Cold/Dry	1997, 2001, 2003, 2005, 2009, 2010, 2013
Cold/Wet	1998, 1999, 2004, 2012

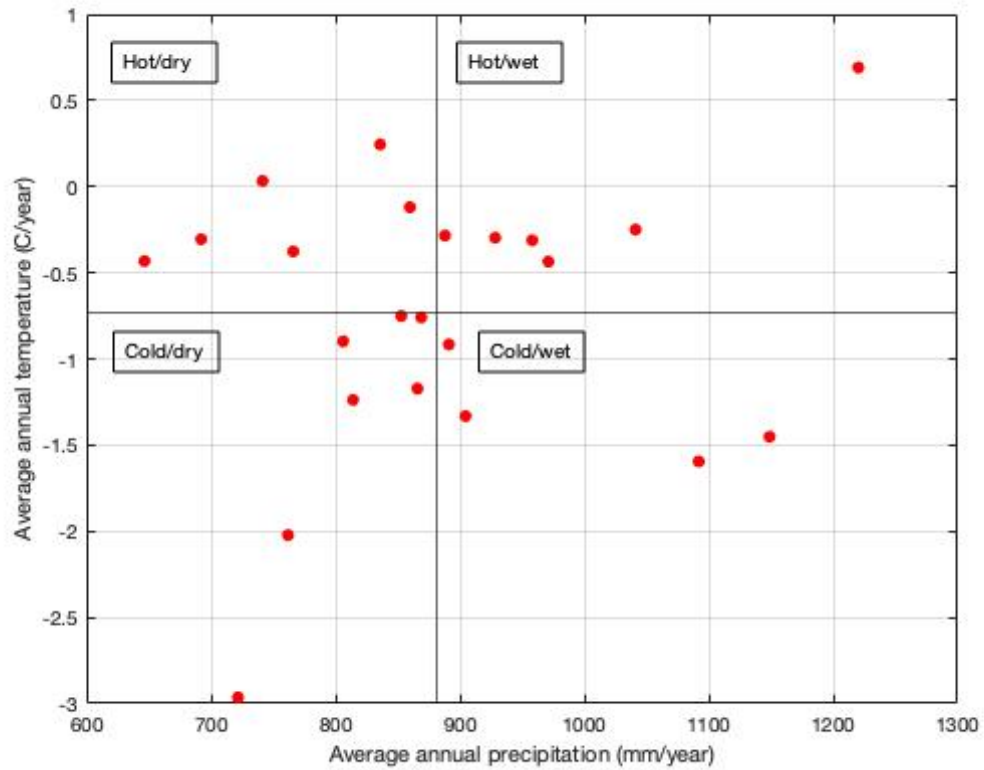Table 7: Sub-periods Yngeredsforsen

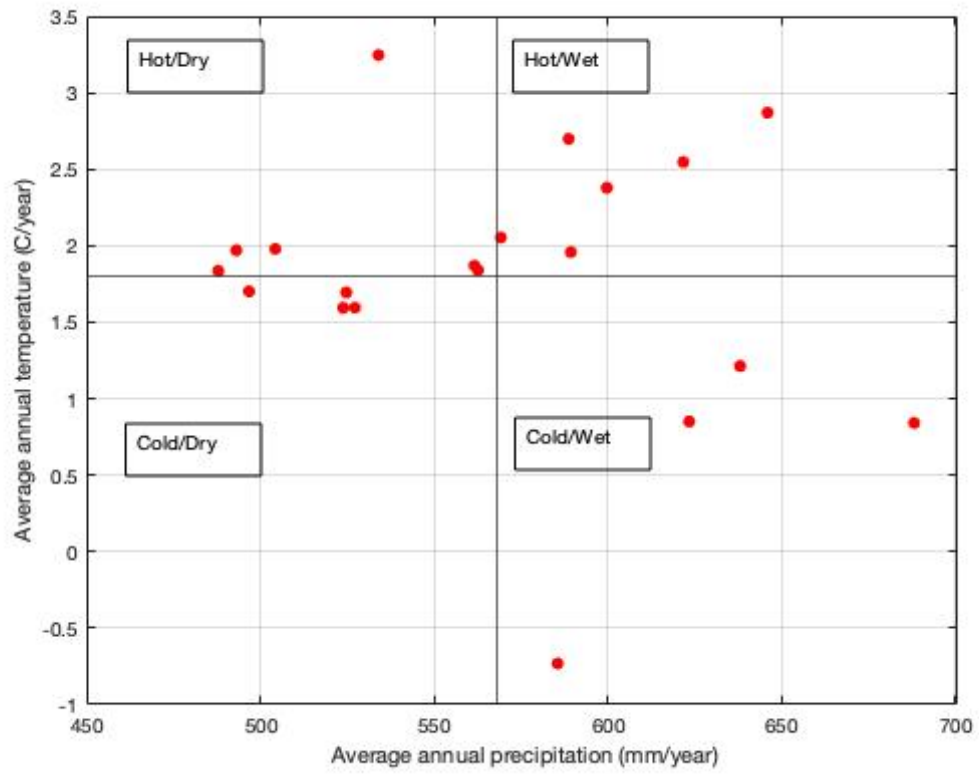Figure 7: Differential split sample test-plot Borgasjön
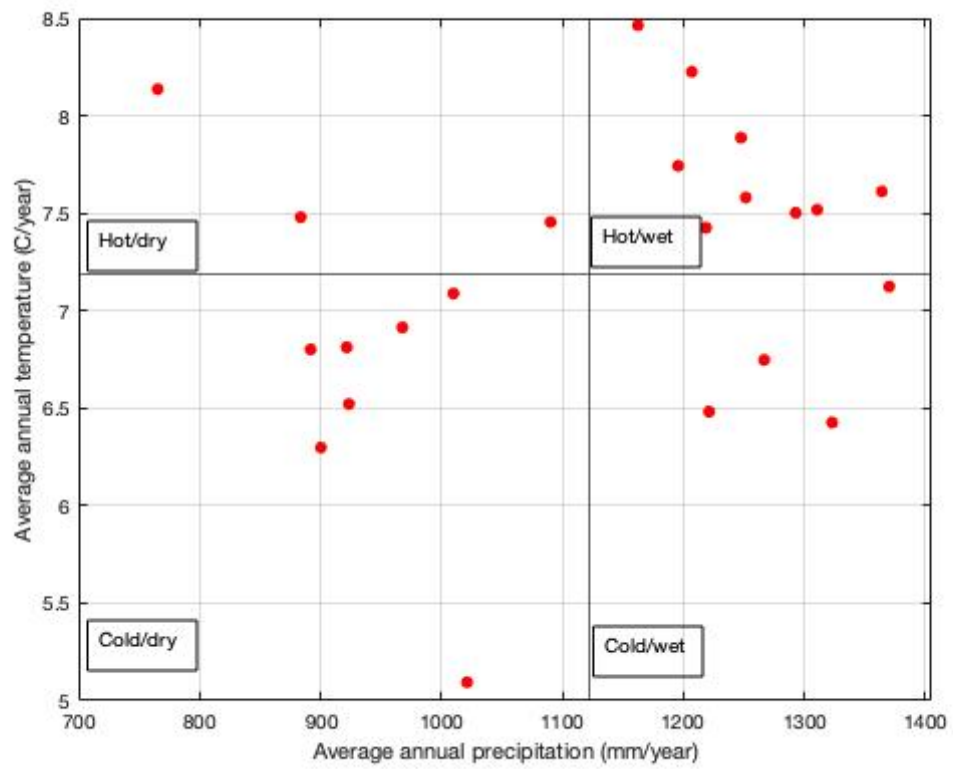
Figure 8: Differential split sample test-plot Lännässjön

Figure 9: Differential split sample test-plot Yngeredsforsen

6.2 Parameters

The optimal range for each parameter were obtained by trial-and-error. At the beginning the parameters were set at a wide range to avoid missing a good parameter set. By running the model the efficiency could be improve by adjusting the lower and upper limits, narrowing the range for each parameter. The obtained parameters are presented in Table 8 and were used for calibration of all catchments. The parameter range were compared with previous studies to make sure that the chosen interval were within similar limits [22], [23].

Parameter	Unit	Lower limit	Upper limit
TT	°C	-2.5	0.8
$CFMAX$	$mm°C^{-1}d^{-1}$	0.3	5
SP	-	0	0
$SFCF$	-	0.4	1
CFR	-	0.05	0.05
CWH	-	0.1	0.1]
FC	mm	80	600
LP	-	0.2	1
$BETA$	-	1	6
$PERC$	mm/dt	0	4
UZL	mm	0	70
$K0$	$1/dt$	0.1	0.5
$K1$	$1/dt$	0.01	0.2
$K2$	$1/dt$	5E-5	0.1
$MAXBAS$	dt	1	2.5

Table 8: Interval for parameter setup used during Monte-Carlo simulation for all PET models and catchments

7 Results

7.1 Precipitation and temperature

By using the meteorological data from SMHIs weather stations in and around each catchment, and using the Thiessens-polygon method to give each station a specific weight, the annual precipitation and mean annual temperature could be calculated for each catchment. The results are presented in Figure 10 and Figure 12. The mean monthly variation of precipitation and temperature for each catchment are presented in Figure 11 and Figure 13

From the figures it can be concluded that there is a distinct difference in both precipitation and temperature between each catchment. Yngeredsforsen has the highest total annual

precipitation, except for 2001, with an average annual precipitation of 1122 mm/year. Borgasjön and Lännässjön have a mean annual precipitation of 882 respectively 568 mm/year. Borgarsjön and Yngeredsforsen is the coldest respectively warmest catchments with an average temperature of $-0.7°C$ and $7.2°C$ per year. Lännässjön has an average temperature of $1.8°C$ per year.
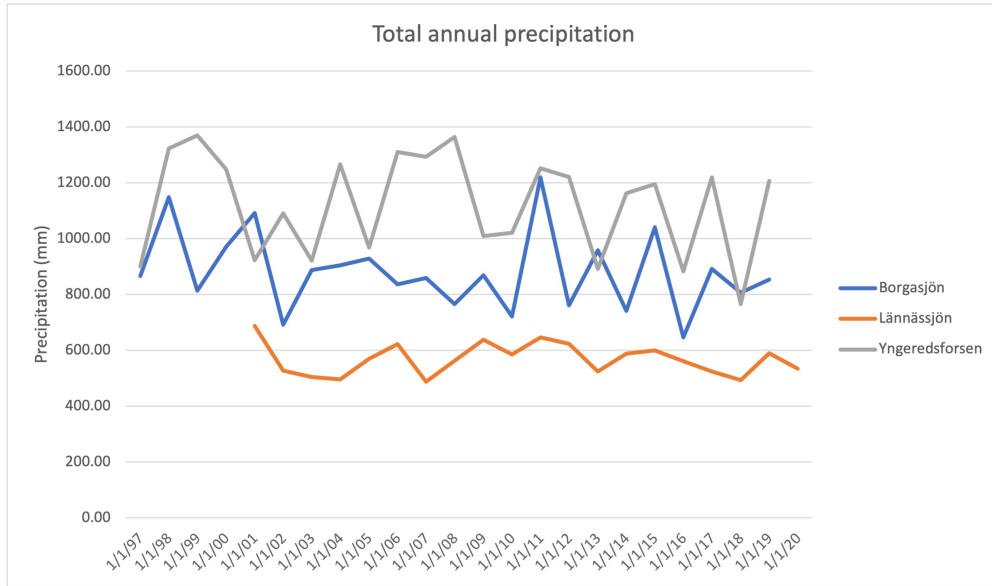

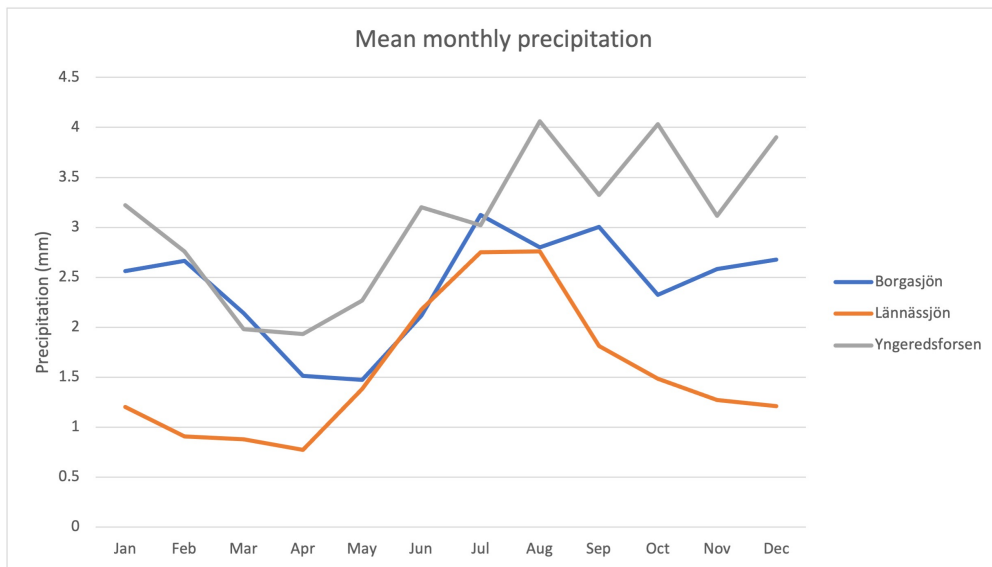Figure 10: Annual precipitation

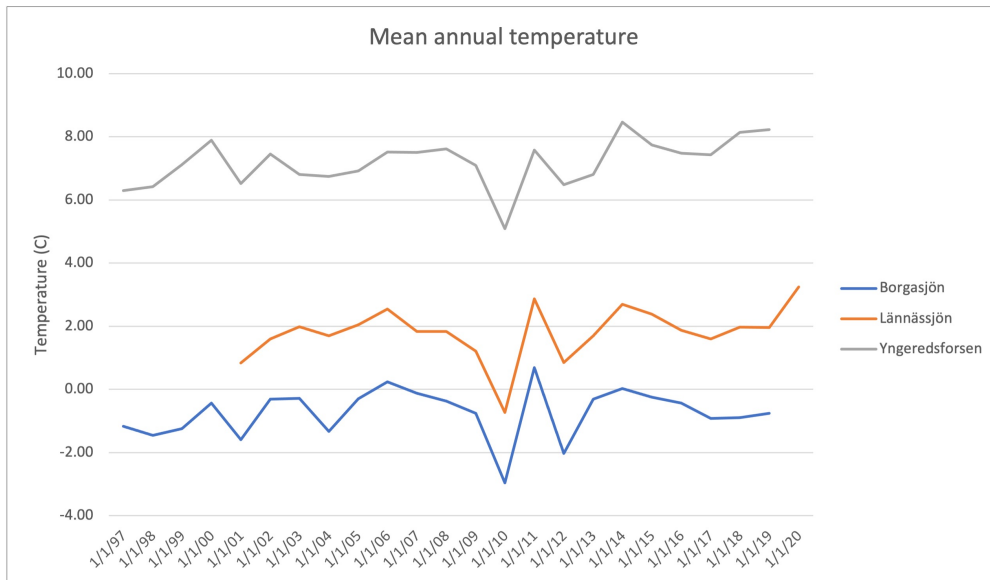Figure 11: Mean monthly precipitation

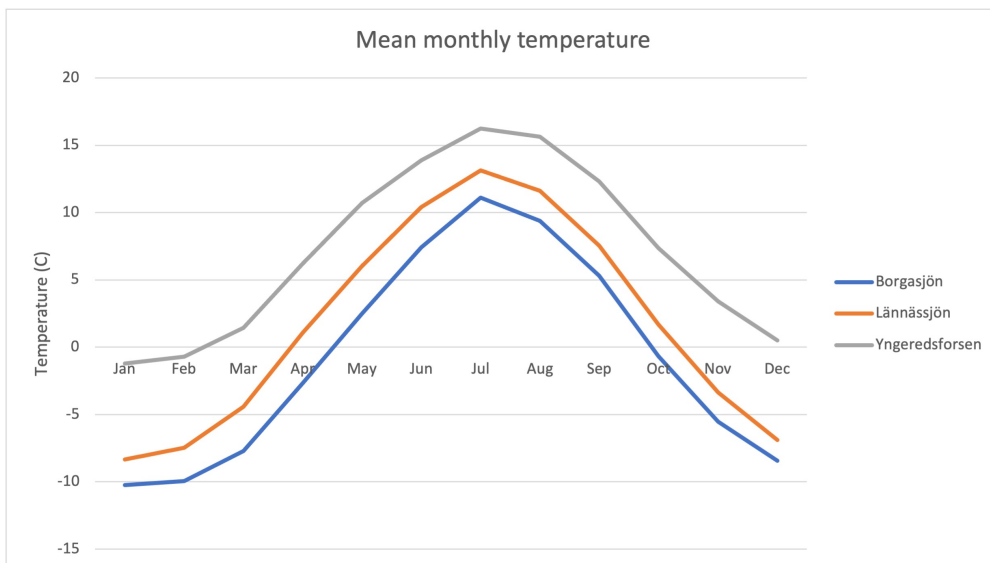Figure 12: Annual temperature

Figure 13: Mean monthly temperature

7.2 Discharge

Figure 14 represents the mean monthly discharge in mm/day for each catchment. It can be noted that both Borgasjön and Lännässjön have their peak in discharge during May to July. Yngeredsforsen have a drier period during summer and sees the biggest flows from December to February.
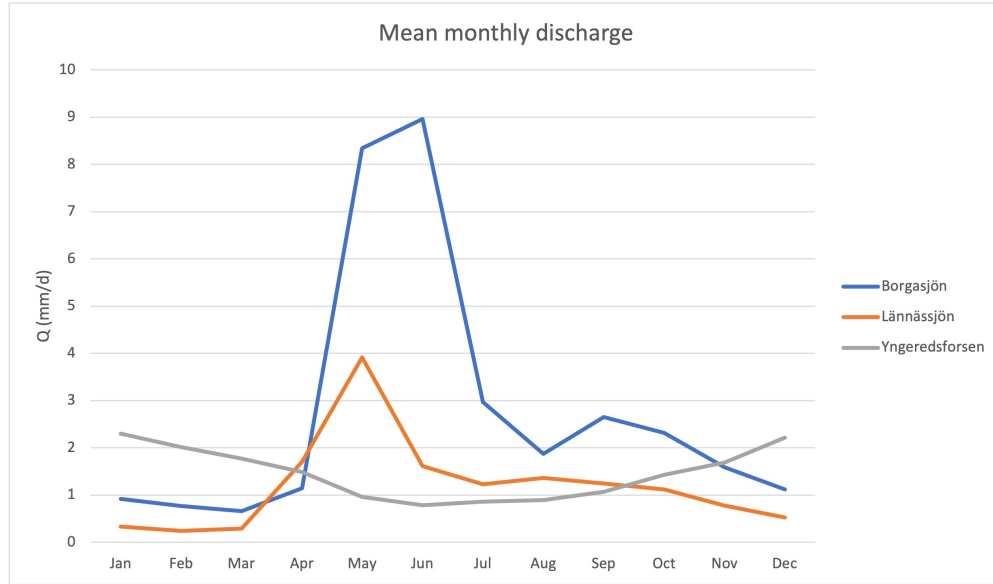

Figure 14: Mean monthly discharge (mm/day)

7.3 Potential evapotranspiration

The total annual PET (mm/year) were calculated for the different PET models and for each catchment, and the results are presented in Figure 15, 16 and 17. Average annual PET (mm/year) for the whole measurement period and for each PET method and catchment are presented in Table 9. These average values are the sum of the daily PET (mm/day) calculated for each PET model and catchment.

PET model	TW	HS	LIN	JH	PM	MG	Current	Mean
Borgarsjön	437	388	268	391	393	399	217	379
Lännässjön	493	519	413	545	526	509	313	474
Yngeredsforsen	588	650	496	861	520	733	-	641

Table 9: Average annual PET (mm/year) for each PET model and catchment

Data from SMHI shows that the average annual PET for the area around Borgarsjön, Lännässjön and Yngeredsforsen ranges from 200-300, 400-500 respectively 500-700 mm per

year. These values are the yearly mean, obtained by using the Penman-Montheit model with meteorological data from 1961 to 1990 [24].

Borgarsjön shows the lowest annual PET values for all PET models compared with the other two catchments. From Figure 15 it can be concluded that the Linacre model and the current values are the only two with an annual PET below the average. The other models result in similar annual PET values, all above the average. Similarly the Linacre model and the current values gives the lowest annual PET for Lännässjön as well. Yngeredsforsen shows the highest annual PET values for all methods, except for the Penman-Montheit, compared with the other catchments. The range of annual PET between each PET model is the largest for this catchment (Figure 17), where the Jensen-Haise model results in an annual PET of 861 mm/year compared to Linacre with an annual PET of 496 mm/year.
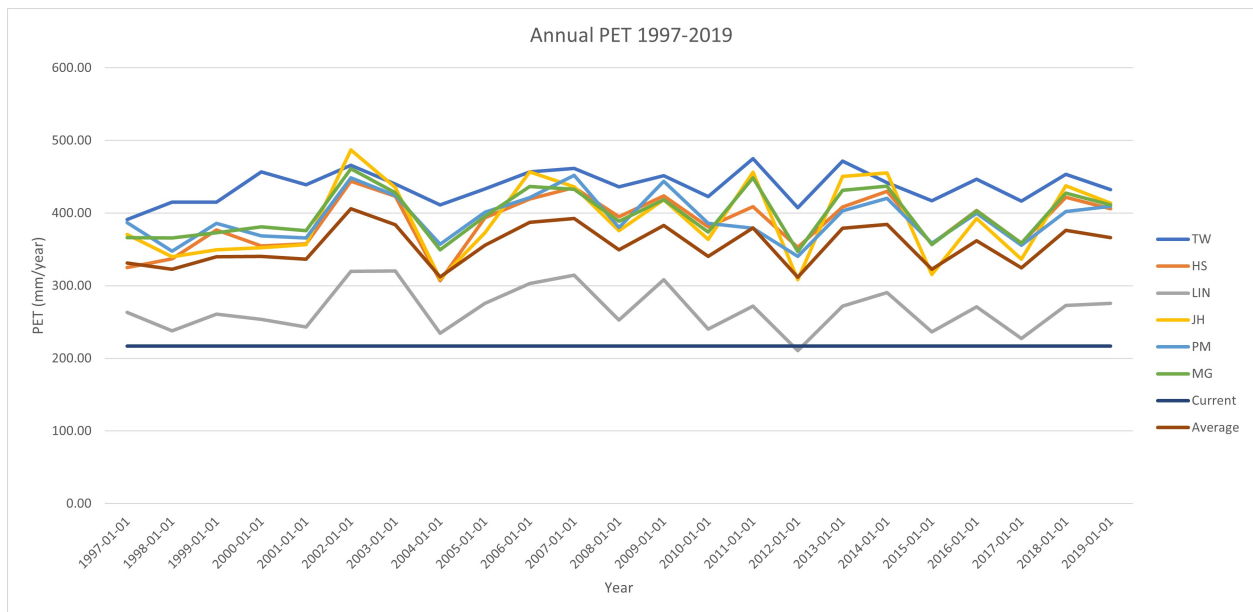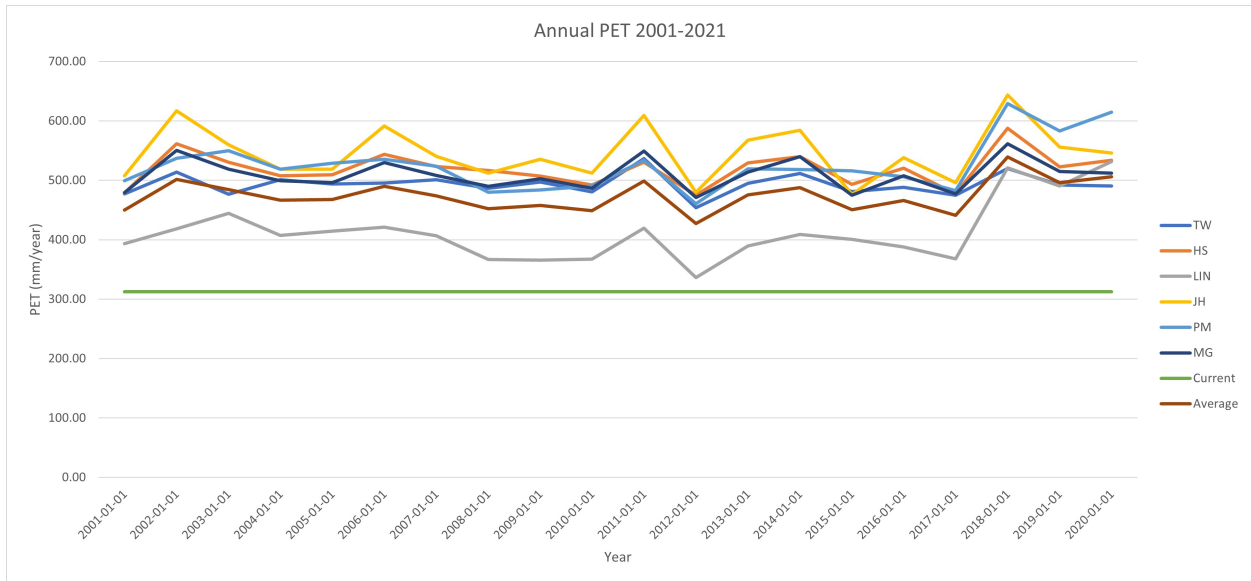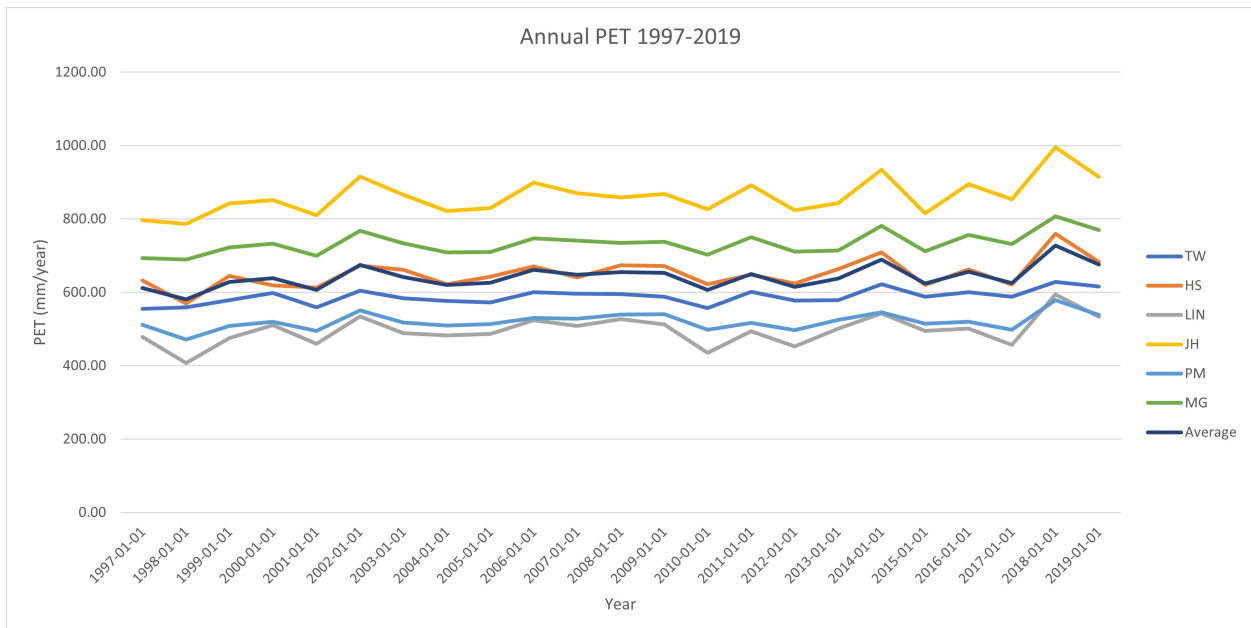

Figure 15: PET Borgasjön

Figure 16: PET Lännässjön

Figure 17: PET Yngeredsforsen

39

7.4 Calibration

The result from the calibration, using KGE as objective function, is presented for each catchment. The result is represented as the average of the 100 parameter set with the highest KGE value for each sub-period and PET model. The volume error for each PET model and the average efficiency for each sub-period is also presented for each catchment.

7.4.1 Borgasjön

Figure 18 shows the KGE for the PET models calibrated on Borgasjön. Using the current values as PET input gives the highest efficiency for all sub-periods, with an average KGE of 0.74. The lowest efficiency for all sub-periods is obtained when the Jensen-Haise model is used, with an average KGE of 0.66. This proves that there is a big difference in efficiency depending on which PET model that's been used.

The volume error for each PET model is presented in Figure 19. Similarly to the efficiency, the current values gives the smallest volume error with an average VE of 0.89 and the Jensen-Haise model gives the biggest volume error with an average VE of 0.77. The average, max and min efficiency and average volume error for all PET models is presented in Table 10.

PET-model	KGE_{ave}	KGE_{Max}	KGE_{Min}	VE_{ave}
HS	0.69	0.76	0.59	0.81
JH	0.66	0.77	0.53	0.77
LIN	0.72	0.78	0.63	0.85
MG	0.68	0.76	0.55	0.79
PM	0.70	0.78	0.61	0.82
TW	0.68	0.75	0.56	0.79
Current	0.74	0.80	0.67	0.89

Table 10: Mean, max and min efficiency for each PET model Borgasjön

The average efficiency and volume error for each sub-period is presented in Table 11. When calibrated on HW the highest efficiency is obtained with an average of KGE 0.71. The smallest volume error is obtained when calibrated on HD with an average of VE 0.84.

Sub-period	KGE	VE
HW	0.71	0.83
HD	0.68	0.84
CW	0.69	0.78
CD	0.70	0.82

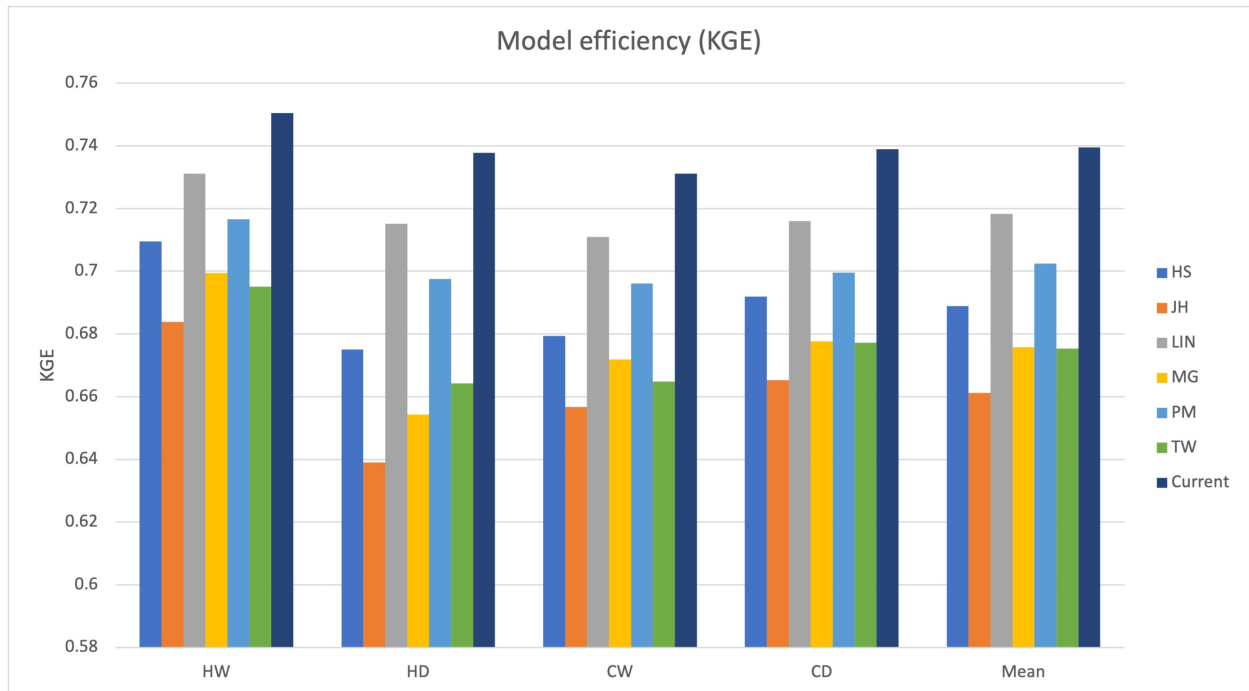Table 11: Mean efficiency for each sub-period Borgasjön

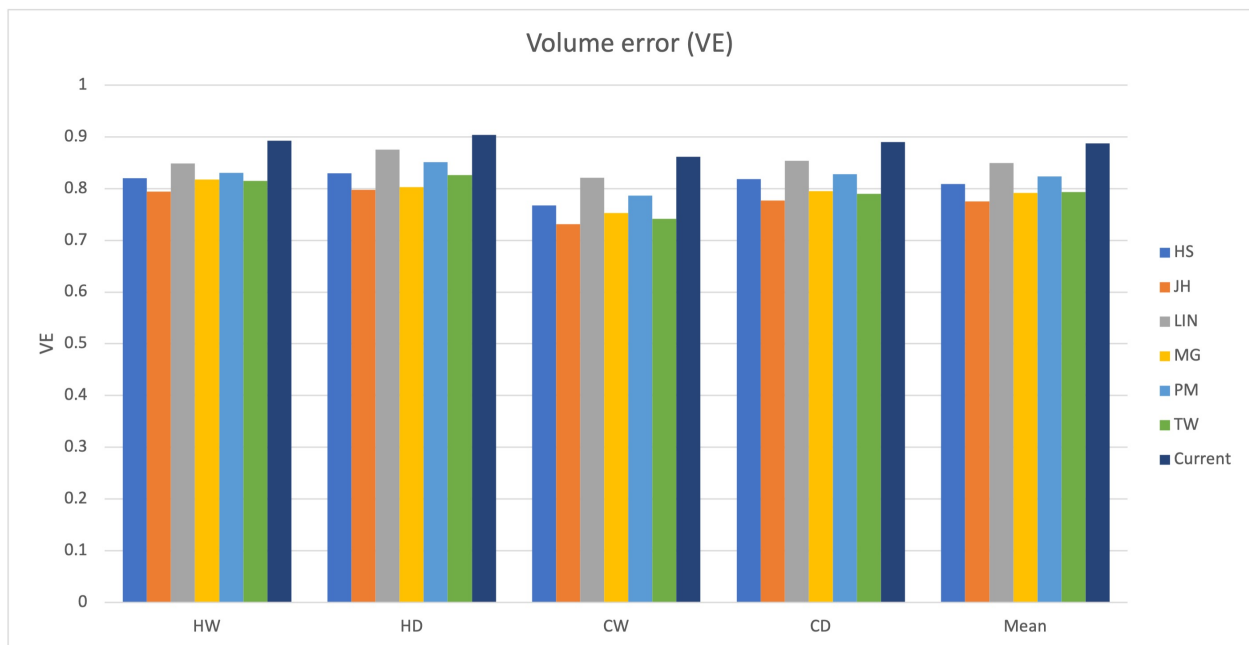Figure 18: Kling-Grupta efficiency Borgasjön

Figure 19: Volume error Borgasjön

7.4.2 Lännässjön

Figure 20 shows the KGE for the PET models calibrated on Lännässjön. The Penman-Monteith model gives the highest average efficiency with an average KGE of 0.86. When calibrated on HW and HD, the Hargreaves-Samani and the Thornthwaite model gives the highest efficiencies, with an average KGE of 0.85 respectively 0.85. The lowest efficiency for all sub-periods is obtained when the current values are used, with an average KGE of 0.70. The average efficiency between each PET model is within a range of $0.80 - 0.86$, if the current values are not considered.

The volume error for each PET model is presented in Figure 21. Similarly to the efficiency, the Penman-Monteith model gives the smallest volume error with an average VE of 0.97 and the current values gives the biggest volume error with an average VE of 0.83. The average, max and min efficiency and average volume error for all PET methods is presented in Table 12.

PET-model	KGE_{ave}	KGE_{Max}	KGE_{Min}	VE_{ave}
HS	0.85	0.91	0.83	0.96
JH	0.80	0.89	0.56	0.94
LIN	0.80	0.87	0.75	0.93
MG	0.85	0.90	0.83	0.95
PM	0.86	0.90	0.83	0.97
TW	0.83	0.88	0.67	0.95
Current	0.75	0.80	0.68	0.83

Table 12: Mean, max and min efficiency for each PET model Lännässjön

The average efficiency and volume error for each sub-period is presented in Table 13. When calibrated on CW the highest efficiency is obtained with an average of KGE 0.82. The smallest volume error is obtained when calibrated on HD with an average of VE 0.94.

Sub-period	KGE	VE
HW	0.81	0.93
HD	0.81	0.94
CW	0.82	0.93
CD	0.81	0.93

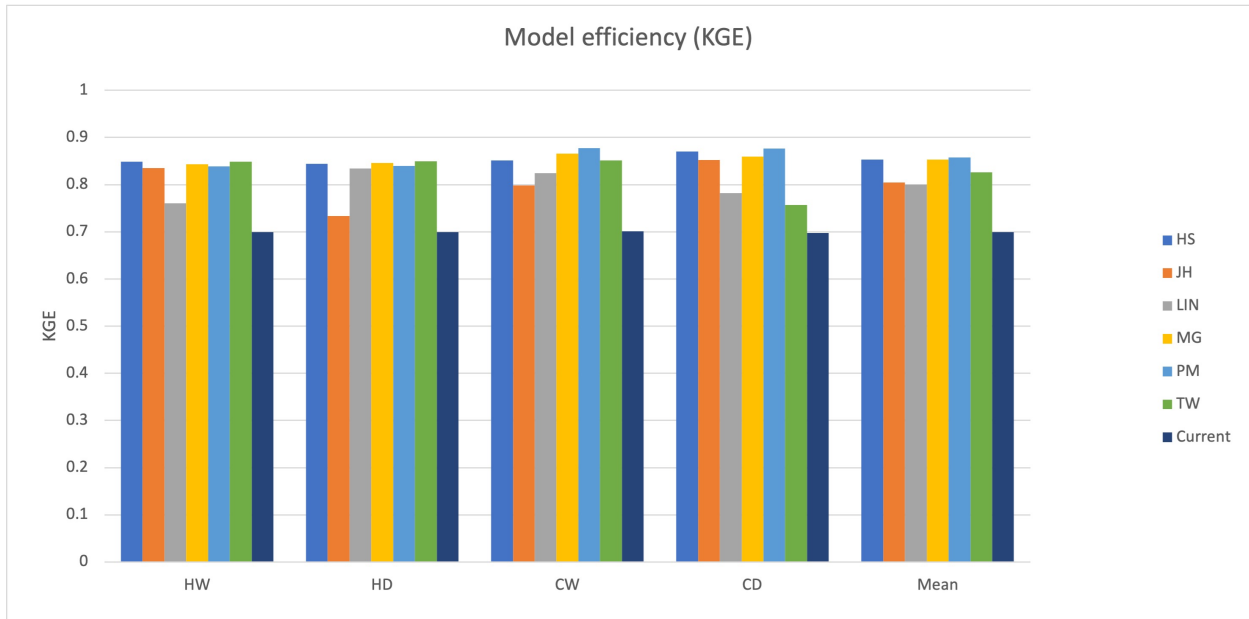Table 13: Mean efficiency for each sub-period Lännässjön

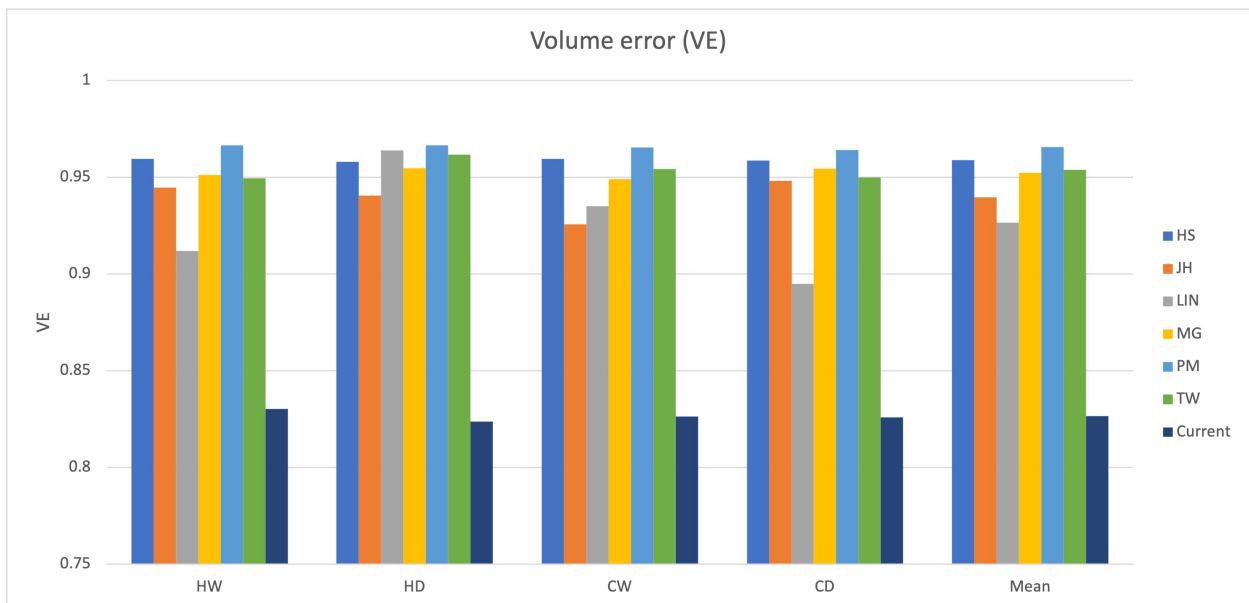Figure 20: Kling-Grupta efficiency Lännässjön

Figure 21: Volume error Lännässjön

7.4.3 Yngeredsforsen

Figure 22 shows the KGE for the PET models calibrated on Yngeredsforsen. The Jensen-Haise model gives the highest average efficiency for all sub-periods, with an average KGE of 0.79. The lowest efficiency for all sub-periods is obtained when the Linacre model is used, with an average KGE of 0.53. The Penman-Monteith model and the McGuinness model also shows poor efficiency with an average KGE of 0.55 respectively 0.55.

The volume error for each PET model is presented in Figure 23. Similarly to the efficiency, the Jensen-Haise model gives the smallest volume error with an average VE of 0.94 and the Linacre model gives the biggest volume error with an average VE of 0.60. The average, max and min efficiency and average volume error for all PET models is presented in Table 14.

PET-model	KGE_{ave}	KGE_{Max}	KGE_{Min}	VE_{ave}
HS	0.73	0.82	0.62	0.84
JH	0.79	0.87	0.58	0.94
LIN	0.53	0.61	0.0006	0.60
MG	0.55	0.66	-0.0096	0.63
PM	0.55	0.65	-0.0365	0.63
TW	0.68	0.76	0.55	0.76

Table 14: Mean, max and min efficiency for each PET model Yngeredsforsen

The mean efficiency and volume error for each sub-period is presented in Table 15. When calibrated on HW the highest efficiency is obtained with an average of KGE 0.67. The smallest volume error is obtained when calibrated on HW with an average of VE 0.74.

Sub-period	KGE	VE
HW	0.67	0.74
HD	0.61	0.73
CW	0.64	0.73
CD	0.63	0.72

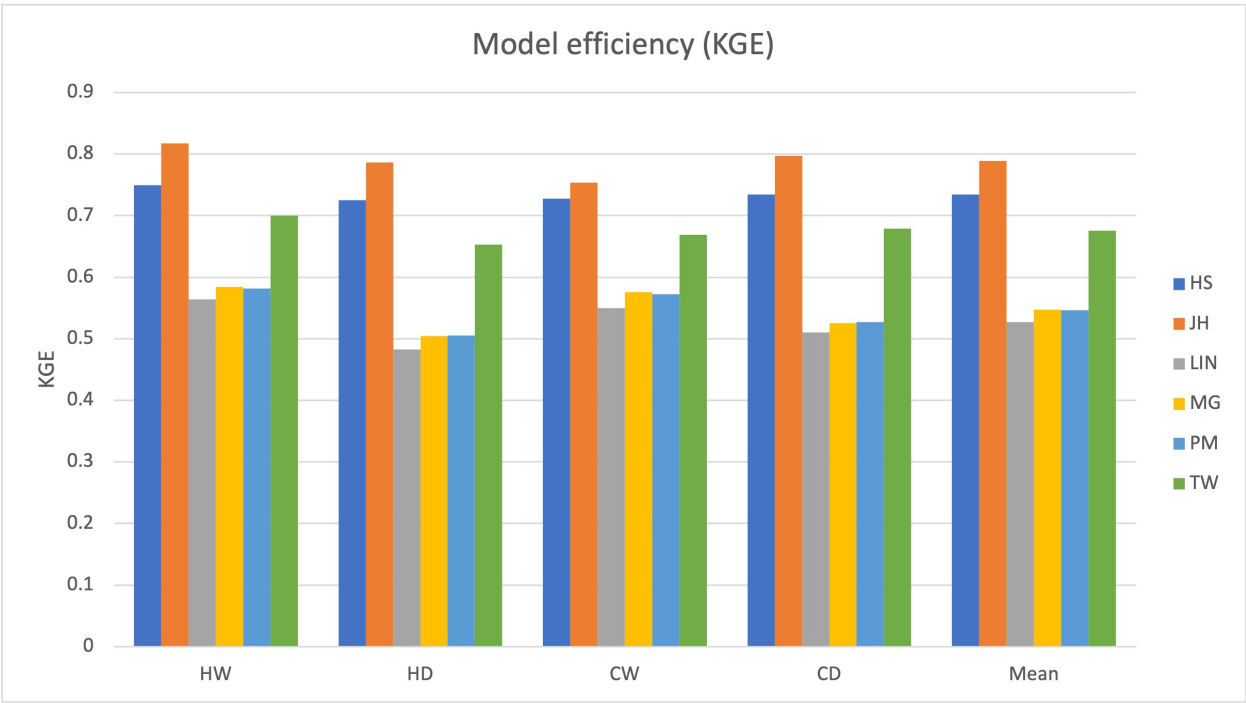Table 15: Mean efficiency for each sub-period Yngeredsforsen

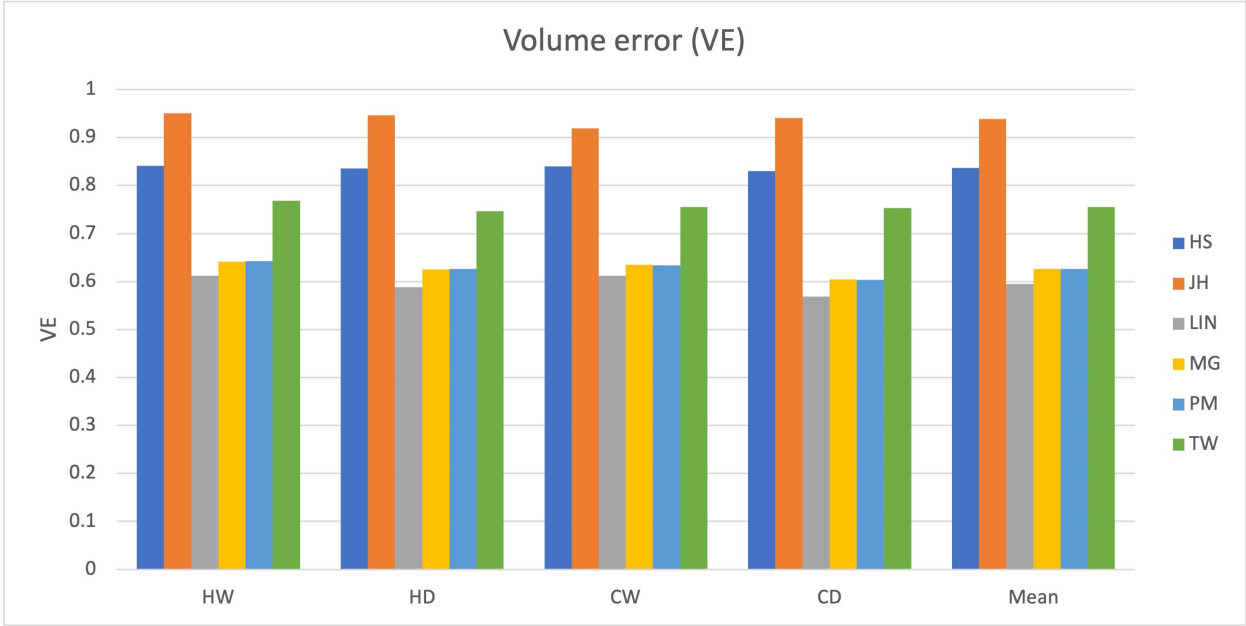Figure 22: Kling-Grupta efficiency Yngeredsforsen

Figure 23: Volume error Yngeredsforsen

7.4.4 General

Figure 24 shows the average KGE for each PET model calibrated over the different sub-periods and catchments. Three PET models shows an acceptable efficiency for all catchments: The Hargreaves-Samani model with an average KGE between $0.69-0.85$, the Jensen-Haise model with an average KGE between $0.66-0.80$ and the Thornthwaite model with an average KGE between $0.68-0.83$. Lännässjön is the catchment with the highest average KGE for all PET models (0.81). Yngeredsforsen shows the lowest average KGE of 0.64.
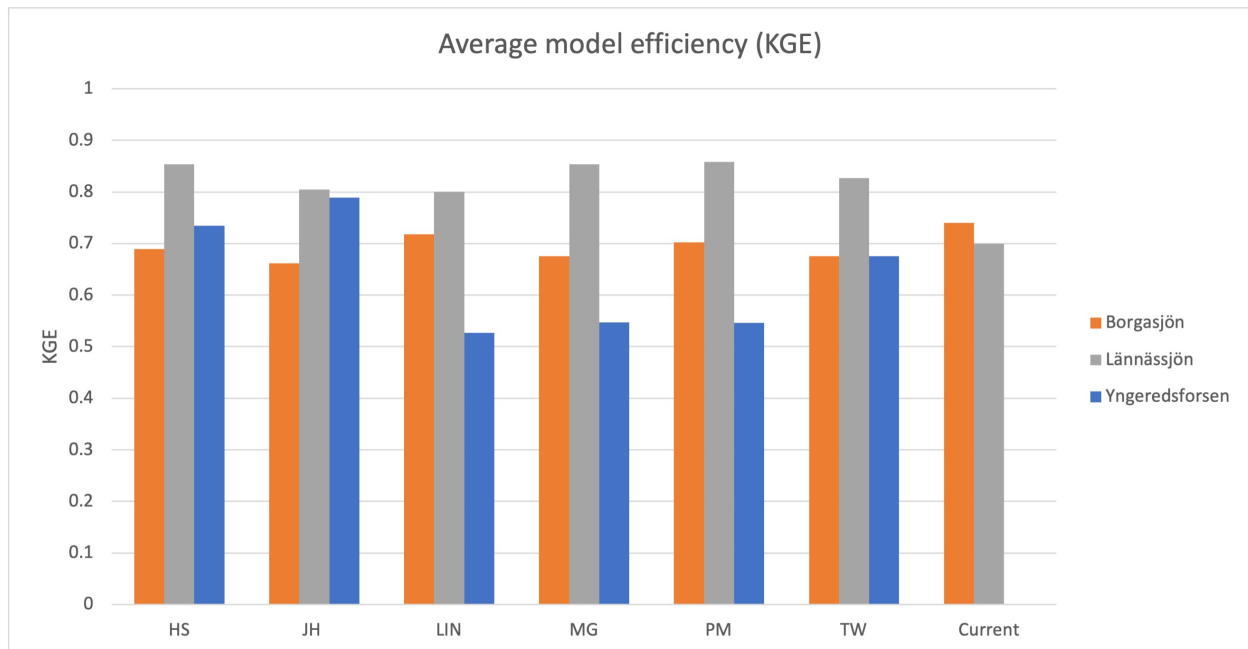

Figure 24: Average efficiency for all calibrations

Figure 25 shows the average VE for the different PET models and for the different catchments. The Hargreaves-Samani model and the Jensen-Haise model shows an acceptable volume error for all catchments ranging between $0.81-0.96$ respectively $0.78-0.94$. Lännässjön shows the lowest average volume error of all the catchments (0.93) and Yngeredsforsen shows the highest (0.73).

Interesting is the low performance of efficiency for the Linacre, McGuinness and Penman-Montheit model for Yngeredsforsen. They show an average KGE of 0.53, 0.55 respectively 0.55. The Annual PET for the McGuinness model is 733 mm/year (Table 9) which is well above the Annual PET for the Hargreaves-Samani and Thornthwaite method (650 mm/year respectively 588 mm/year). They both show a higher efficiency, which suggests that the McGuinness method is poor when it comes to estimating PET for Yngeredsforsen.

Table 16 shows the mean efficiency for calibration on each sub-period. Calibration on HW shows the highest mean efficiency for both Borgarsjön and Yngeredsforsen. The difference in
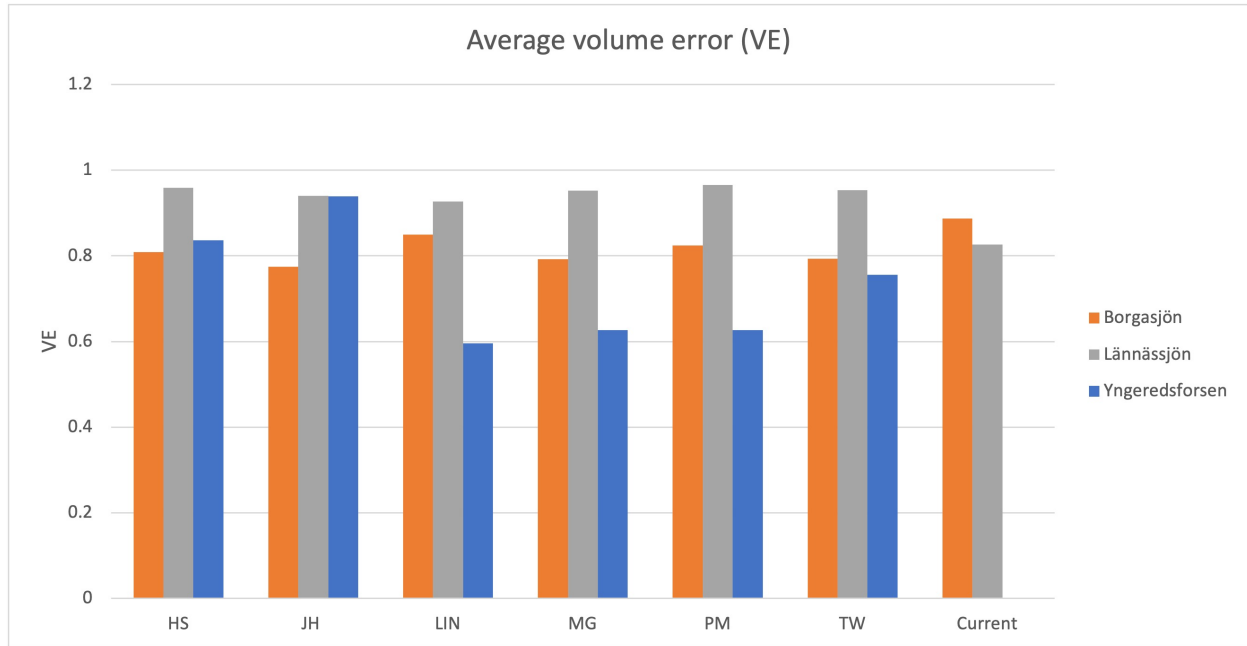
Figure 25: Average volume error for all calibrations

efficiency between each sub-period is not that big for any catchments, the biggest difference is obtained for Yngeredsforsen between calibration on HW and HD (0.06).

Catchment	HW	HD	CW	CD
Borgasjön	0.71	0.68	0.69	0.70
Lännässjön	0.81	0.81	0.82	0.81
Yngeredsforsen	0.67	0.61	0.64	0.63

Table 16: Mean efficiency for calibration on each sub-period

Table 17 shows which sub-period that provides the parameter set with highest efficiency during calibration for each PET model and catchment. Calibration on HD and HW for Borgasjön shows the highest efficiencies for all PET models. This is interesting as Borgasjön is the catchment with the lowest average temperature (Figure 12). For Lännässjön calibration on CD and CW provides the highest efficiencies.

PET model	Borgasjön$_{max}$	Lännässjön$_{max}$	Yngeredsforsen$_{max}$
HS	HD	CD	CW
JH	HW	CD	HW
LIN	HD	CW	CW
MG	HW	CW	CD
PM	HD	CW	CW
TW	HD	CD	HW
Current	HD	HW	-

Table 17: Sub-periods providing the max KGE for each PET model and catchment

7.5 Validation

The result from the validation is presented for each catchment. The 100 parameter sets obtained from the calibration of each PET model and sub-period were validated over the other sub-periods and the whole reference period. The result is represented as the average NSE of all the validations for one sub-period and PET model. The volume error for each PET model and the mean efficiency for each sub-period is also presented for each catchment.

7.5.1 Borgasjön

Figure 26 shows the NSE for the PET models validated on Borgasjön. The current values as PET input results in the highest mean NSE of 0.51. The highest overall NSE (0.57) is obtained for the Penman-Montheit model calibrated on CW. The lowest mean NSE is obtained when using the Jensen-Haise model, with a value of 0.45. The lowest overall NSE (0.31) is obtained for the Jensen-Haise model calibrated on HD.

Figure 27 shows the volume error obtained for each PET model. The current PET values shows the smallest VE for all sub-periods. The mean efficiency and volume error for all PET models is presented in Table 18.

PET-model	NSE_{ave}	VE_{ave}
HS	0.47	0.81
JH	0.45	0.78
LIN	0.50	0.85
MG	0.45	0.79
PM	0.50	0.82
TW	0.45	0.79
Current	0.51	0.89

Table 18: Mean efficiency and volume error for each PET model Borgasjön

The mean efficiency and volume error for each sub-period is presented in Table 19. For all PET models the highest NSE is obtained when calibrated on CW, ranging from a NSE of $0.56 - 0.57$. Calibration on HD shows the lowest NSE for all PET models. When calibrated on CW all PET models shows the largest VE.

Sub-period	KGE	VE
HW	0.48	0.83
HD	0.37	0.86
CW	0.56	0.76
CD	0.49	0.82

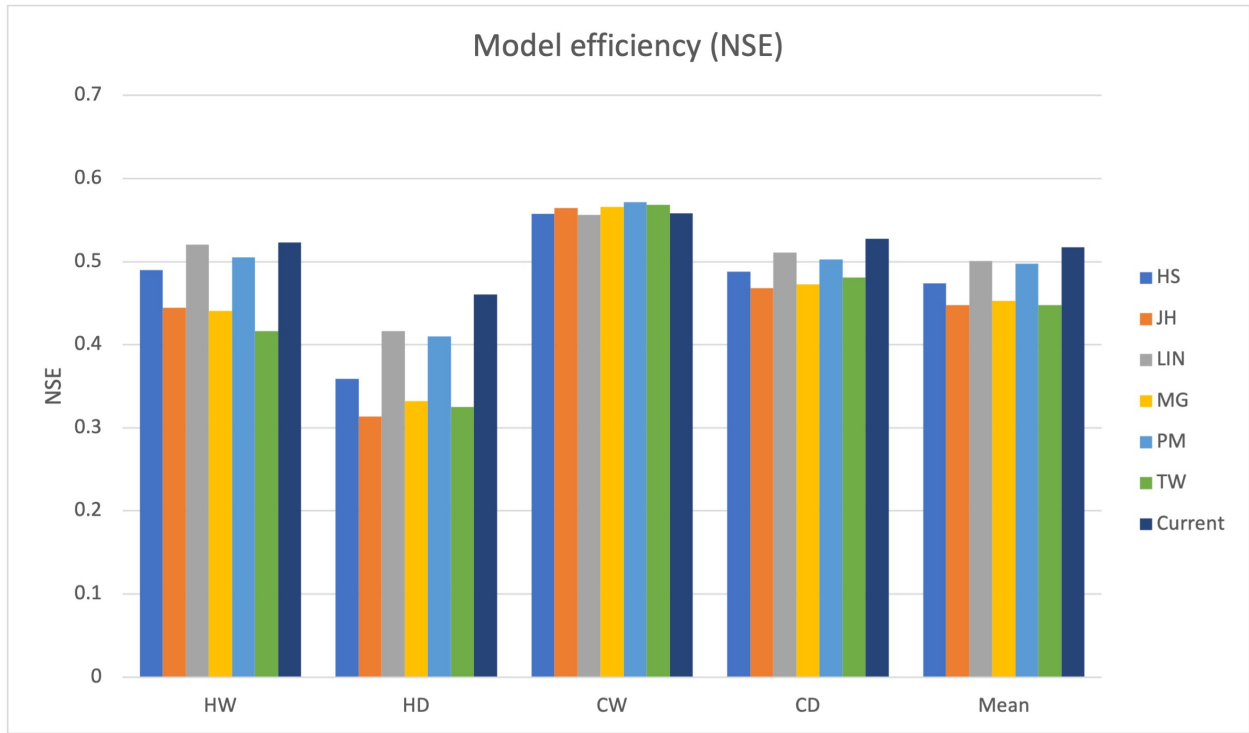Table 19: Mean efficiency for each sub-period Borgasjön
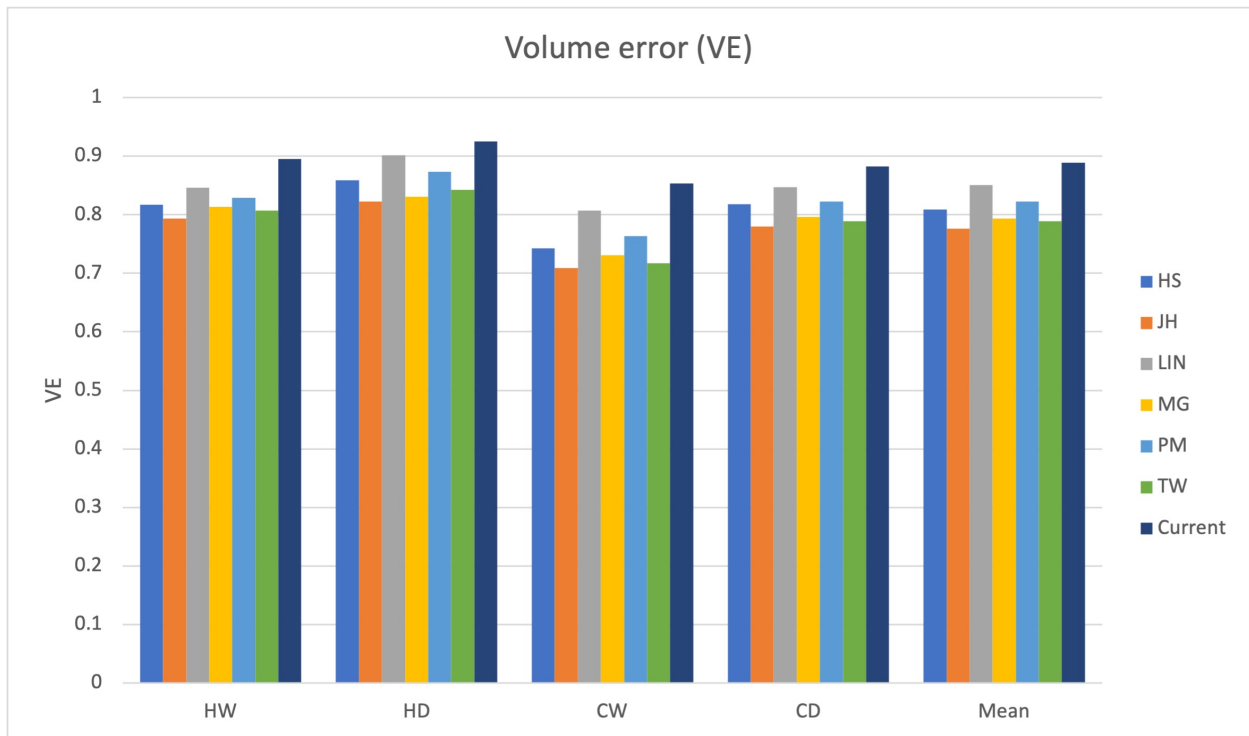
Figure 26: Model efficiency (NSE) Borgasjön

Figure 27: Volume error Borgasjön

7.5.2 Lännässjön

Figure 28 shows the NSE for the PET models validated on Lännässjön. The Thorntwaite model results in the highest mean NSE of 0.69 and the highest overall NSE (0.70) when calibrated on CD. The lowest mean NSE is obtained when using the Linacre model, with a value of 0.55. The lowest overall NSE (0.53) is obtained for the Linacre model calibrated on CW.

Figure 29 shows the volume error obtained for each PET model. The Thorntwaite model results in the smallest mean volume error of 0.95. The mean efficiency and volume error for all PET models is presented in Table 20.

PET-model	NSE_{ave}	VE_{ave}
HS	0.67	0.94
JH	0.67	0.93
LIN	0.55	0.90
MG	0.63	0.94
PM	0.66	0.93
TW	0.69	0.95
Current	0.55	0.83

Table 20: Mean efficiency and volume error for each PET model Lännässjön

The mean efficiency and volume error for each sub-period is presented in Table 21.

Sub-period	KGE	VE
HW	0.65	0.92
HD	0.63	0.92
CW	0.61	0.91
CD	0.64	0.91

Table 21: Mean efficiency for each sub-period Lännässjön
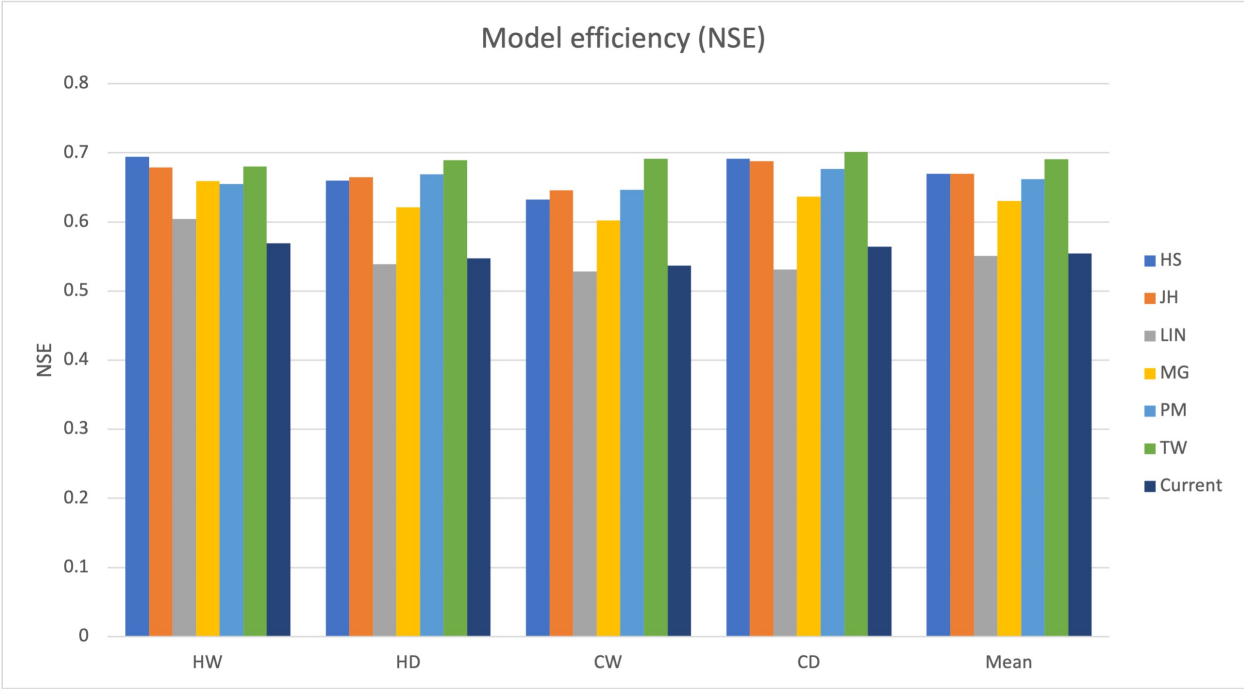
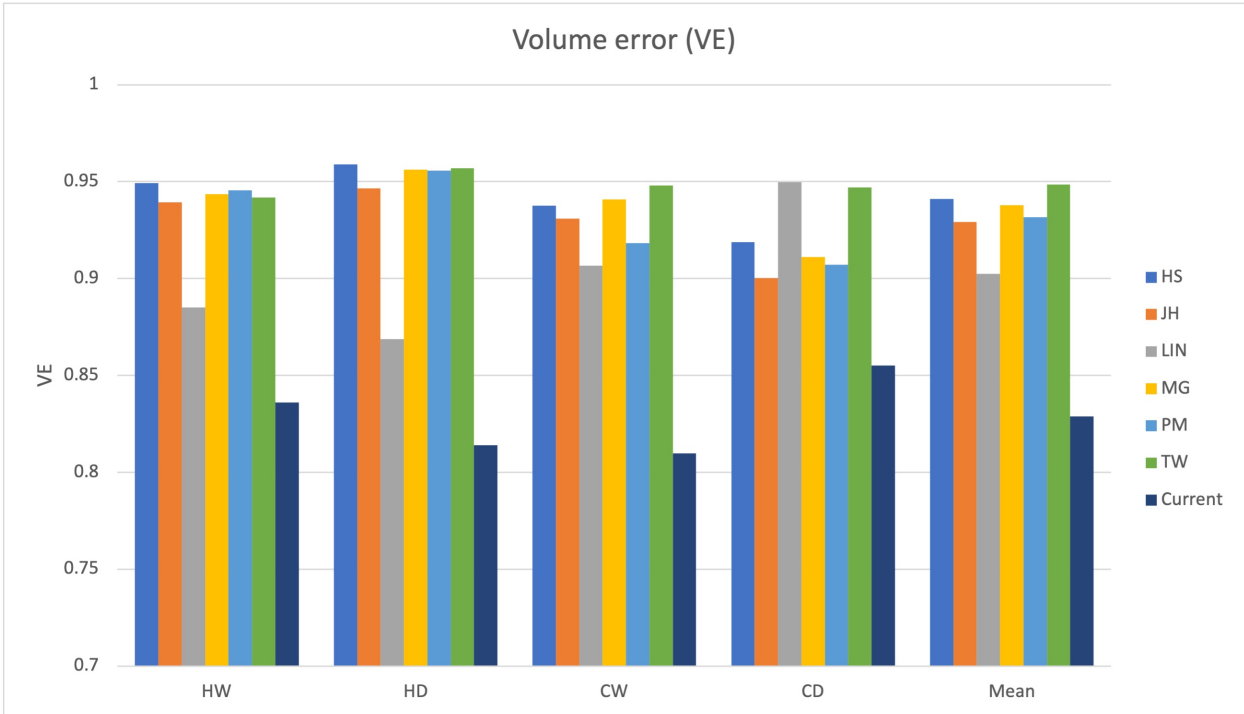Figure 28: Model efficiency (NSE) Lännässjön

Figure 29: Volume error Lännässjön

7.5.3 Yngeredsforsen

Figure 30 shows the NSE for the PET models validated on Yngeredsforsen. The Jensen-Haise model results in the highest mean NSE of 0.62 and the highest overall NSE (0.67) when calibrated on CD. The lowest mean NSE is obtained when using the Linacre model, with a value of 0.08. The lowest overall NSE (−0.11) is obtained for the Linacre model calibrated on HD.

Figure 31 shows the volume error obtained for each PET model. The Jensen-Haise model results in the smallest mean volume error of 0.94. The mean efficiency and volume error for all PET models is presented in Table 22.

PET-model	NSE_{ave}	VE_{ave}
HS	0.57	0.84
JH	0.62	0.94
LIN	0.08	0.56
MG	0.22	0.61
PM	0.22	0.61
TW	0.49	0.76

Table 22: Mean efficiency and volume error for each PET model Yngeredsforsen

The mean efficiency and volume error for each sub-period is presented in Table 23. Calibration on CW and CD shows the highest NSE for all PET models.

Sub-period	KGE	VE
HW	0.36	0.70
HD	0.26	0.74
CW	0.41	0.71
CD	0.43	0.73

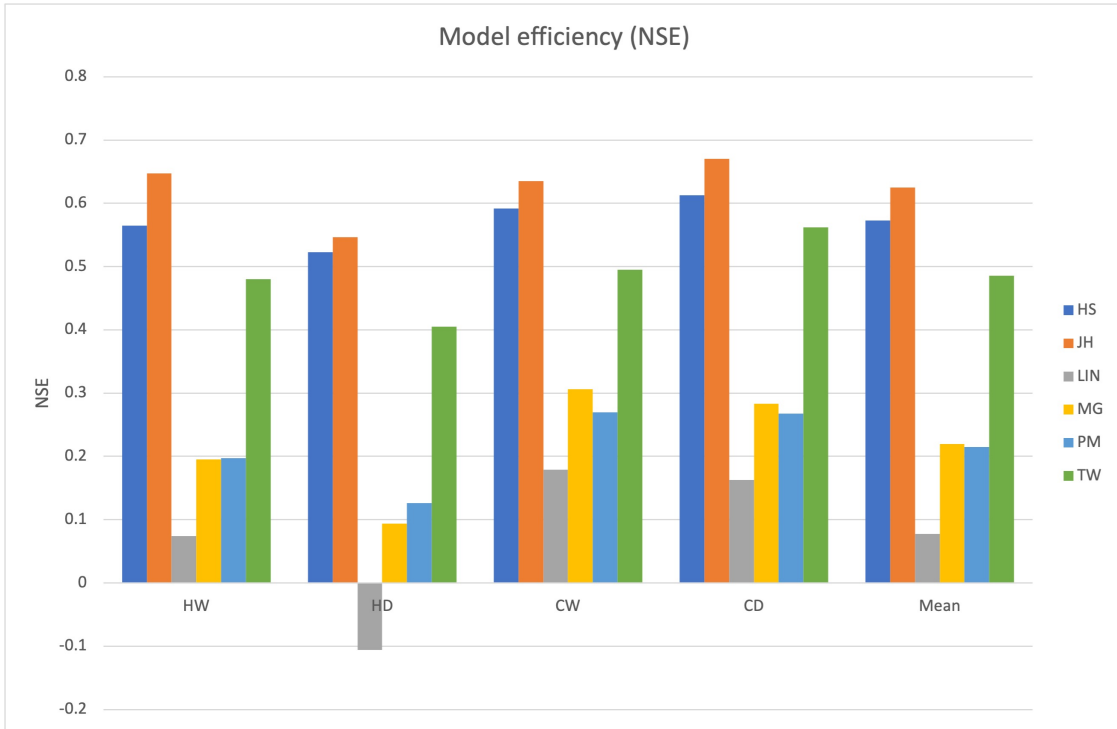Table 23: Mean efficiency for each sub-period Yngeredsforsen

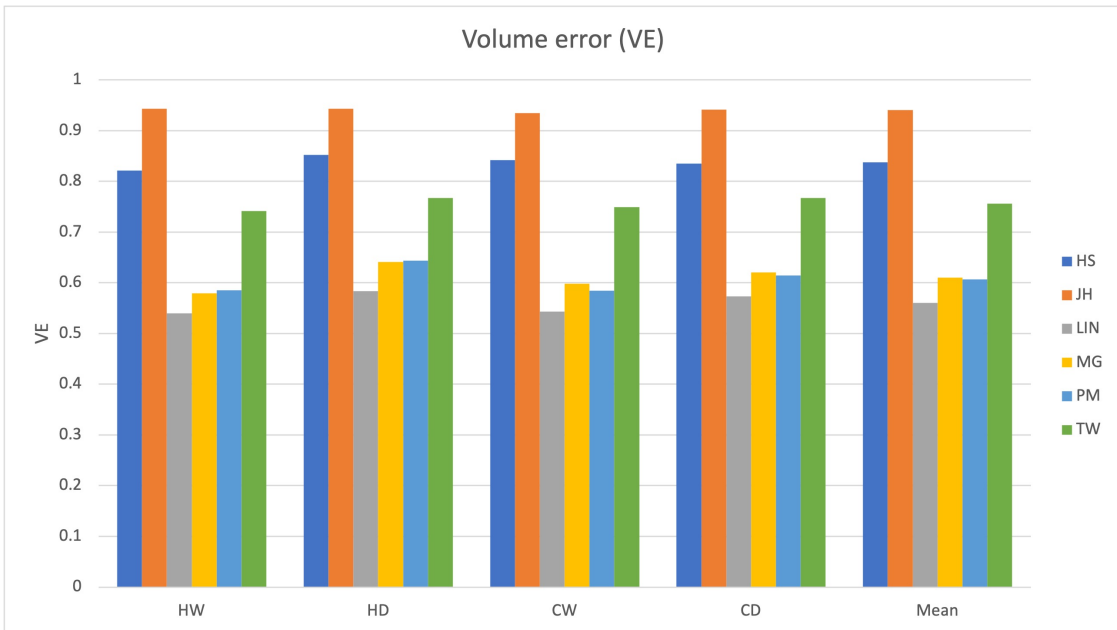Figure 30: Model efficiency (NSE) Yngeredsforsen

Figure 31: Volume error Yngredsforsen

7.5.4 General

Figure 32 shows the average NSE for the different PET models validated over all sub-periods and the whole reference period. Two PET models shows an acceptable efficiency for all catchments: The Hargreaves-Samani model with an average NSE between $0.49 - 0.67$ and the Jensen-Haise model with an average NSE between $0.47 - 0.67$. Lännässjön is the catchment with the highest average NSE for all PET models (0.63) where as Yngeredsforsen shows the lowest average NSE of 0.37.
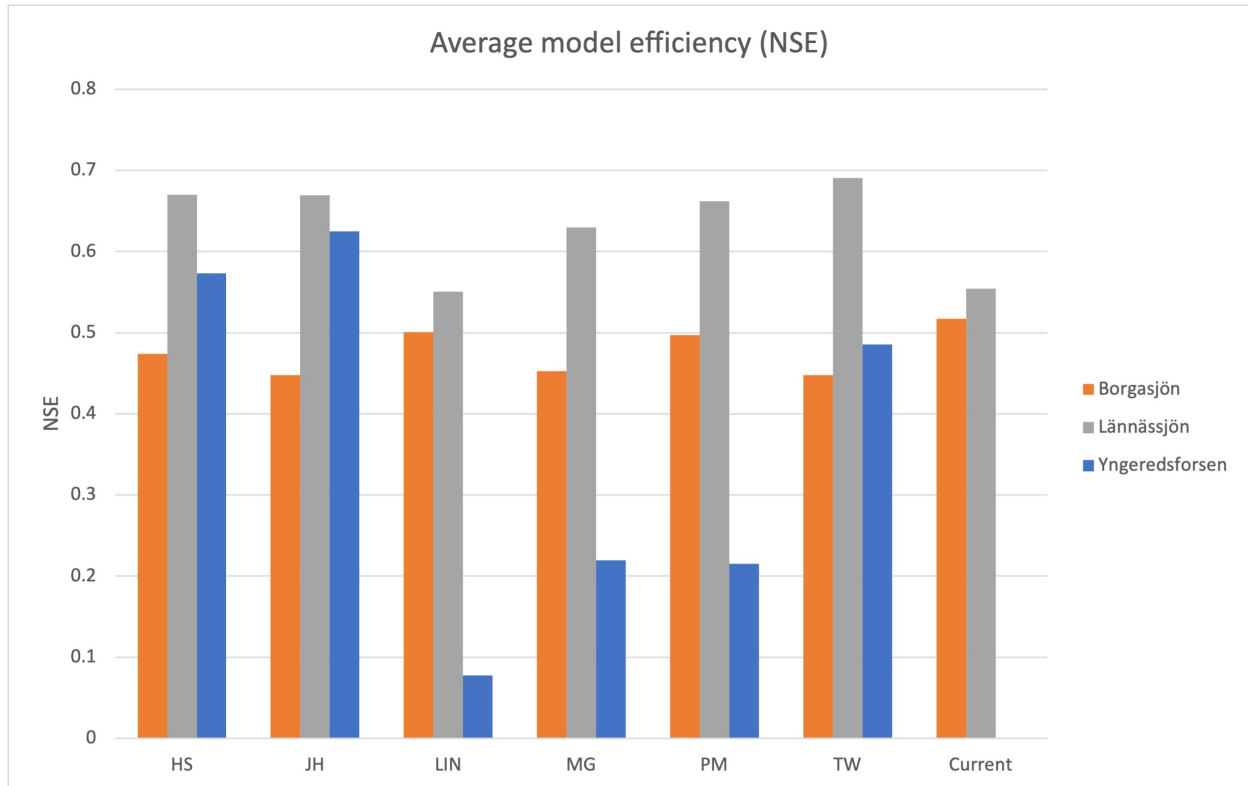

Figure 32: Average efficiency for all validations

Figure 33 shows the average VE for the different PET models and for the different catchments. The Hargreaves-Samani model and the Jensen-Haise model shows an acceptable volume error for all catchments ranging between $0.82 - 0.94$ respectively $0.78 - 0.94$. Lännässjön shows the lowest average volume error of all the catchments (0.92) and Yngeredsforsen shows the highest (0.72).

The previous figures show the validation of each PET model as the average efficiency for all sub-periods. Figure 34 shows the average efficiency when validated on the whole reference period only. This is relevant as the reference period represents the whole historic conditions. A small increase in efficiency can be observed for all PET models.

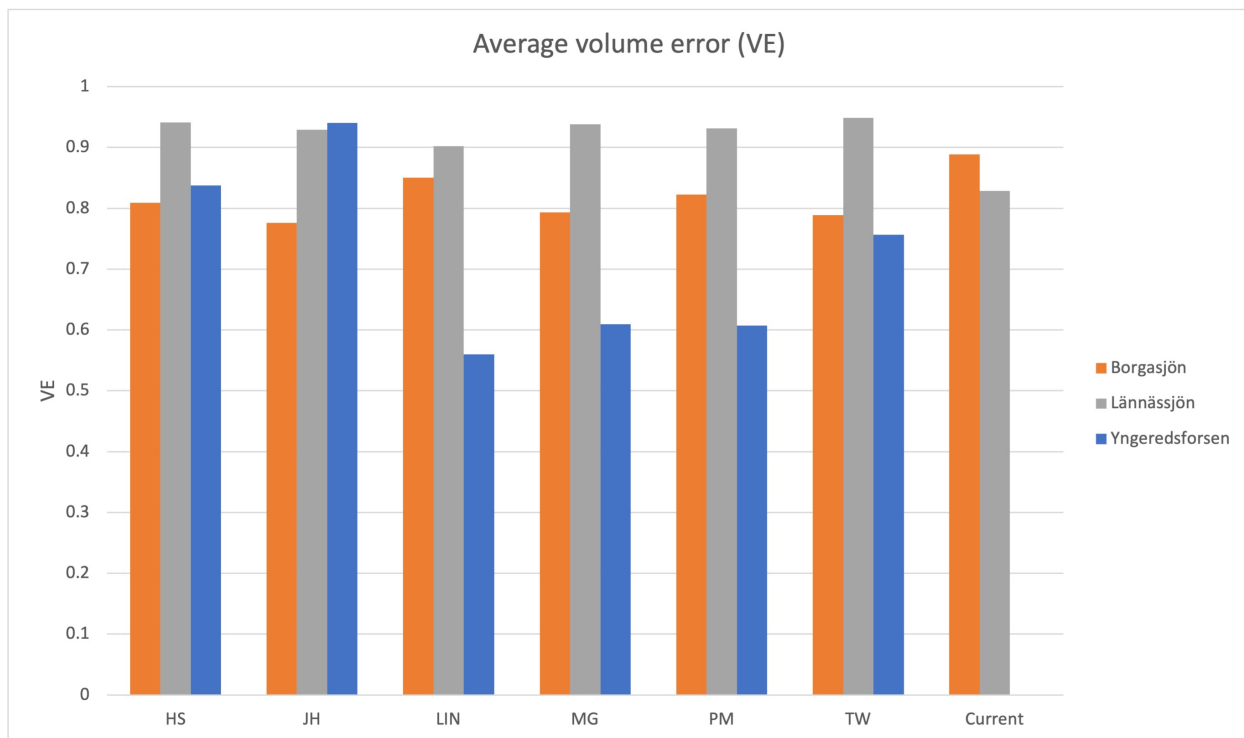Table 24 shows the mean efficiency for validation of each sub-period. Validation of parame-

Figure 33: Average volume error for all validations

ters calibrated on CW shows the highest mean efficiency for both Borgarsjön and Yngeredsforsen. The difference in efficiency between each sub-period is not that big for Lännässjön. But for Borgarsjön and Yngeredsforsen the biggest difference is obtained between CW and HD (0.19) respectively between CD and HD (0.17).

Catchment	HW	HD	CW	CD
Borgasjön	0.48	0.37	0.56	0.49
Lännässjön	0.65	0.63	0.61	0.64
Yngeredsforsen	0.36	0.26	0.41	0.43

Table 24: Mean efficiency for validation of each sub-period

From Figure 26 it can be observed that for Borgasjön all PET models shows the highest NSE when calibrated on CW, and the lowest when calibrated on HD. For Yngeredsforsen there is a slightly higher NSE for all PET models when calibrated on CW or CD (Figure 30), and a lower efficiency when calibrated on HD. For Lännässjön there is no remarkable difference in NSE for calibration on the different sub-periods.
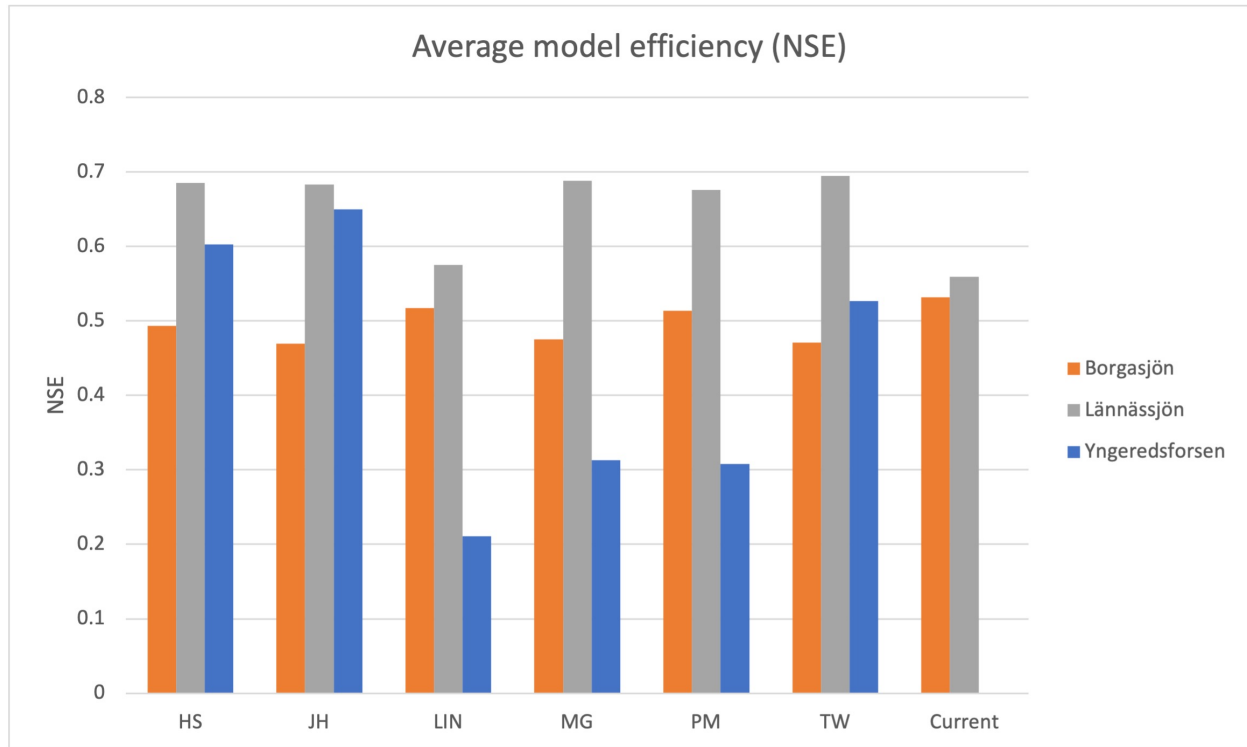
Figure 34: Average efficiency for validation on whole reference period only

7.6 Parameter uncertainty

The parameters describe the physical properties which vary for each catchment and conditions, were some parameters are more sensitive than others. If the chosen interval is to narrow there is a risk that potential parameter sets with high efficiency will be lost. But if the interval is to wide there is also a risk to miss efficient parameter sets due to the increased number of sets that can be generated.

For this thesis the same parameter interval (Table 8) were used for all catchments and PET models. Figure 35 and Figure 36 shows the distribution of each parameter for the 100 parameter sets with the highest KGE, generated with the Hargreaves-Samani model as PET input over the Lännässjön catchment.

Here it can be noted that the parameters describing the snow routine (TT, CFMAX, SFCF) are not that sensitive as they are varying within a smaller interval for all sub-periods. The parameters describing the soil moisture routine (FC, LP, BETA) and the response routine (PERC, UZL, K0, K1, K2, MAXBAS) are on the other hand more sensitive as the vary within a wider range for each sub-period. It can also be noted that for TT, K0 and MAXBAS the lower limit may be to high, and for LP, UZL and MAXBAS the upper limit may be to low. This will probably affect the efficiency negatively as some efficient parameters will be lost.
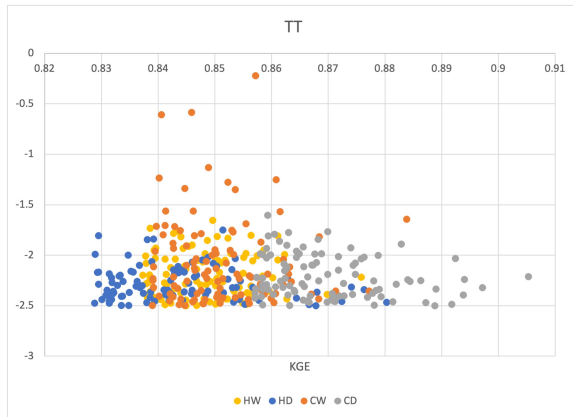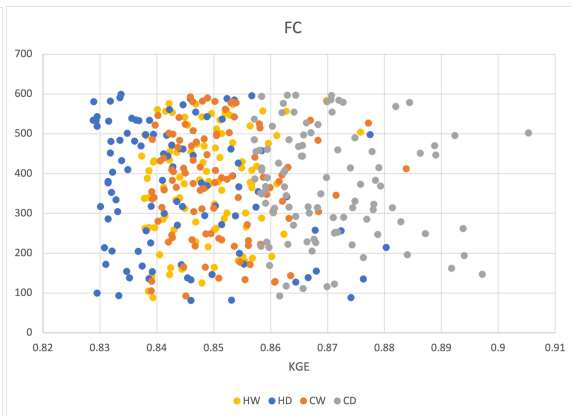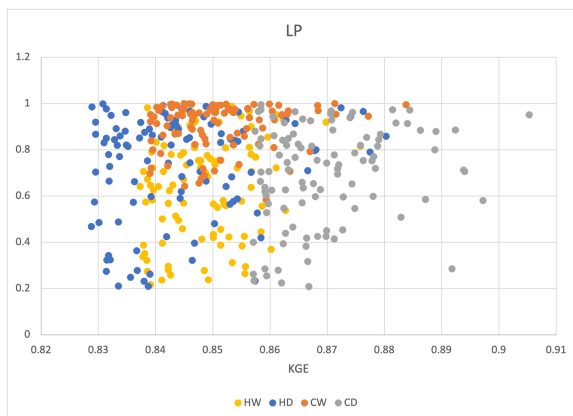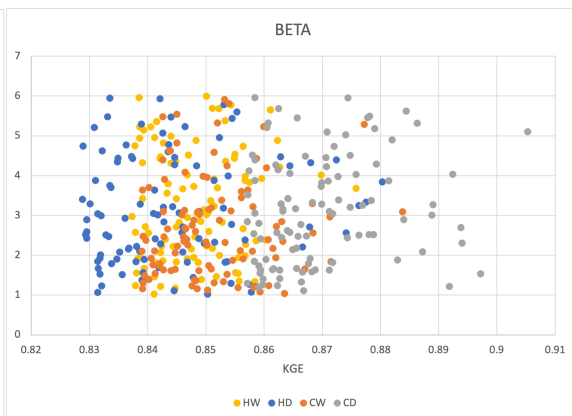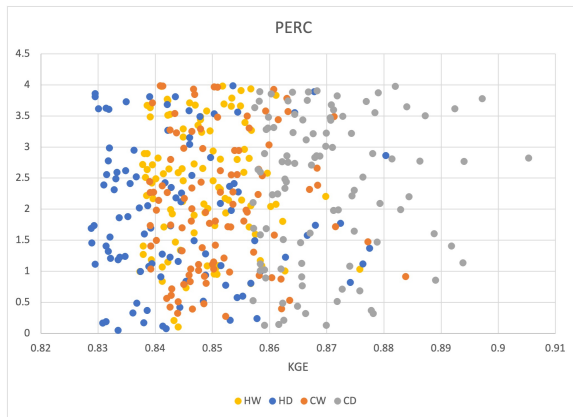
(a) TT
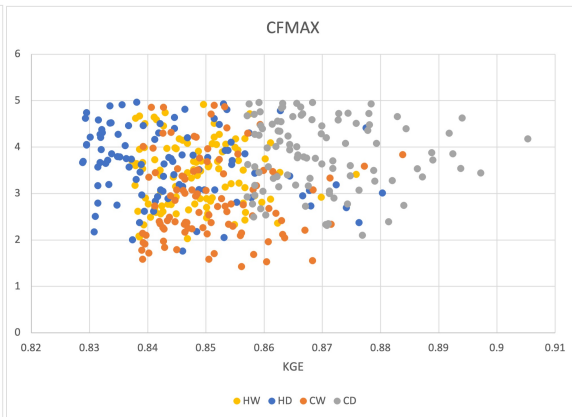
(b) CFMAX
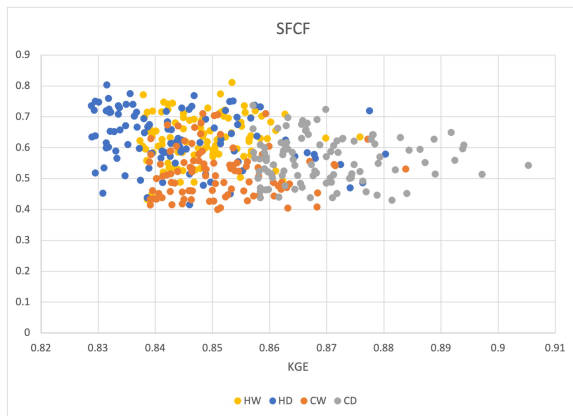
(c) SFCF

(d) FC

(e) LP
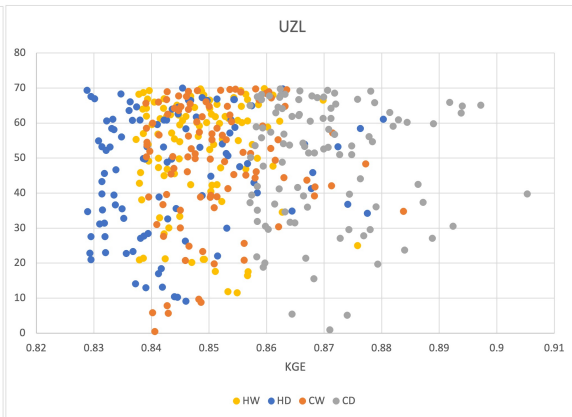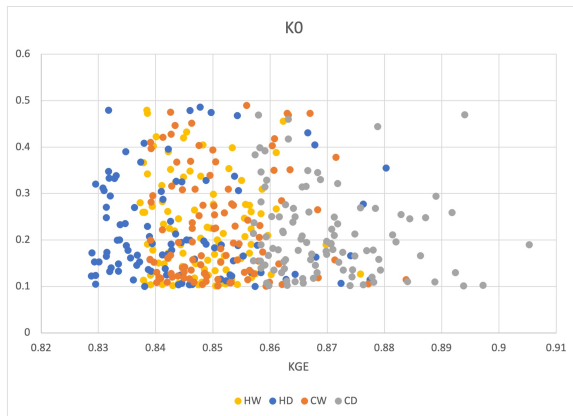
(f) BETA

Figure 35: Plot of the 100 parameter sets with the highest KGE
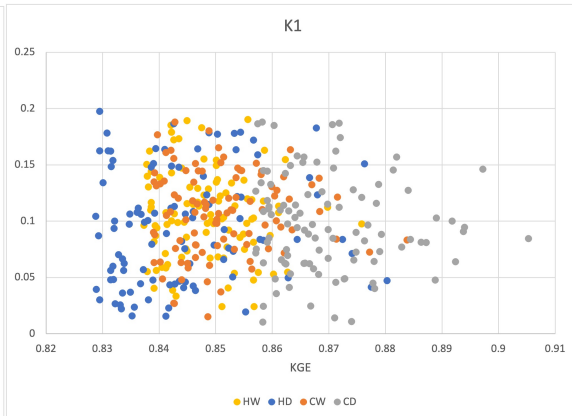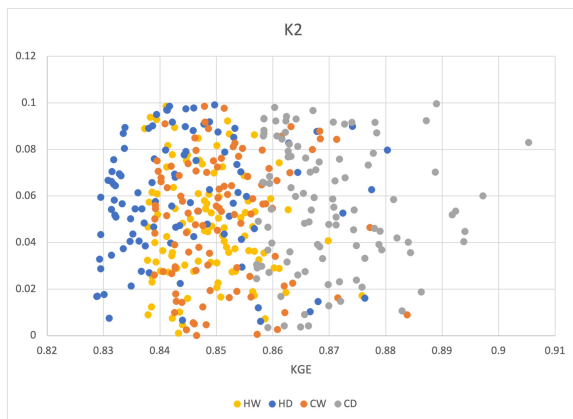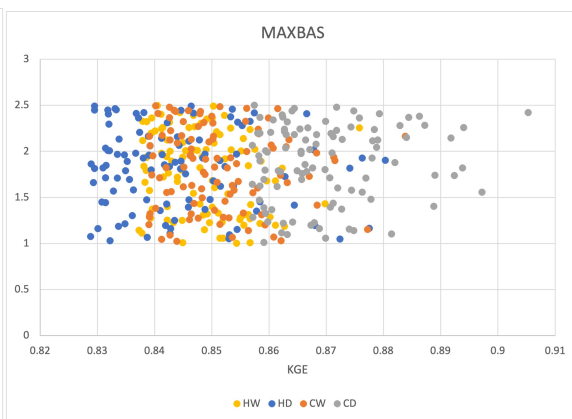
58

(a) PERC

(b) UZL

(c) K0

(d) K1

(e) K2

(f) MAXBAS

Figure 36: Plot of the 100 parameter sets with the highest KGE

59

8 Discussion

The performance in efficiency differs for each catchment where Lännässjön shows the highest efficiency for both calibration and validation for all PET models, followed by Borgasjön and lastly Yngeredsforsen. The decrease in efficiency between calibration and validation for all PET models is largest for Yngeredsforsen and especially for the Linacre, McGuinness or Penman-Montheith model. They show an average KGE of 0.53, 0.55 respectively 0.55 and an average NSE of 0.08, 0.22 respectively 0.22. These models seems more robust for the other two catchments as the decrease in efficiency is much smaller there. One possible conclusion could be that these three models are poor in estimating streamflow when the streamflow is very low. 14 shows that the average monthly streamflow is much lower for Yngeredsforsen compared with the other catchments. The Jensen-Haise and the Hargreaves-Samani model performs better when calibrated and validated over Yngeredsforsen compared to Borgasjön. Looking at 9 it can noted that the estimation of annual PET for the Jensen-Haise and Hargreaves-Samani model are higher compared to the Linacre and Penman-Montheith model for Yngeredsforsen. In search for a connection between high efficiency and estimated annual PET it can be noted that there is no relation between high or low estimations of annual PET and high or low efficiencies. Instead the efficiency must rely more on how the estimated PET is divided over the hydrological year. The PET models were only tested on three catchments with varying results so it can not be concluded if the result applies on a larger variety of catchments. Although the result is pointing at that the selection of PET model seems to be site specific, further analysis is needed in other catchments/regions to confirm this.

The result of this thesis is not in line with the result from previous studies. Oudin et al. found no significant difference in performance between 27 PET models tested on 308 catchments located in Australia, France and the United States, indicating a lack of sensitivity of rainfall runoff models to PET input. Similar to this thesis they found that the best average efficiency was obtained with the Jensen-Haise model and that more complex PET models such as the Penman-Montheit did not improve the efficiency. In the study done by Dakhlaoui et al. it was concluded that discharge simulations are not sensitive to PET estimates when tested over catchments in semi-arid regions.

Why the result from this thesis is different from similar studies may be due to many factors. There are a few uncertainties which needs to be considered for this thesis. One is the credibility of the meteorological data used. Some measurement stations were far away for the catchment (especially for Borgasjön Figure 3) and may therefore not represent the actual meteorological condition. The meteorological data is of key importance as the result from each PET model depend upon its quality. Two measurement stations for each catchment were used for data of temperature and wind speed. By using the mean values from a larger amount of stations it would reduce the risk of using incorrect data. But at the same time it is important to make sure that the distance to each station is within reasonable limits. The radiation-based models and The Penman-Montheith model need data for solar radiation. This could only be obtained at a few meteorological stations in Sweden, for this thesis Östersund and Växjö. These stations are far away from the catchments and would most

likely provide a poor representation of the actual radiation. By using a temperature-based model this uncertainty would be eliminated. The peak of discharge occurs between April to June for Borgasjön and Lännässjön while it occurs between November to February for Yngeredsforsen. In HBV-light the hydrological year is set between the first on January to the end of December. This could be one factor to the low efficiency for Yngeredsforsen, as the chosen hydrological year do not coincide with the discharge peak.

The DSST were used in order to see how well each PET method performed when calibrated and validated over periods with different climatic conditions. Calibration on CW resulted in higher efficiencies for all PET methods for both Borgasjön and Yngeredsforsen. These two catchments varies in both annual temperature, precipitation and discharge, indicating that parameters calibrated on CW periods may result in a higher robustness. Due to the limited number of catchments though, it can not be concluded if some climatic conditions results in higher average efficiencies. In the study done by Dakhlaoui et al. the found that the difference in climate between calibration and validation affects the performance of the model. They used a similar DSST and concluded that the highest efficiency is obtained when the model is calibrated on climatic scenarios similar to the climatic scenarios during validation.

9   Conclusion

The main conclusion of this thesis is that there is a big difference in efficiency between each PET model but also between the catchments. Some PET models could provide acceptable efficiencies in one catchment but perform poorly in another. This points at that the choice of PET model is site specific and that no general PET model could be found. In order to achieve robust models with high efficiencies regarding streamflow a way could be to divide all catchments into different climatic categories, and instead try to find the PET model which works best for each category. The Hargreaves-Samani and the Jensen-Haise model were the two PET models which showed an acceptable performance for both calibration and validation for Lännässjön and Yngeredsforsen. For these catchment the meteorological and hydrological conditions are very unlike, proving that the Hargreaves-Samani and the Jensen-Haise model works well for different conditions. The PET models have only been tested on three catchments with varying results and it can therefore not be concluded if the obtained results actually reflects how well each PET model perform, or if the results is caused by chance. The differential split sample test showed that parameters calibrated on CW resulted in a slightly higher efficiency during validation for both Borgasjön and Yngeredsforsen. This proves that the chosen calibration period is important in providing a robust model and that the parameters are climate dependant. Like previous studies it could be noted that calibration and validation on similar climatic conditions would provide models with higher efficiency.

References

(1) Ajami, H. Geohydrology: Global Hydrological Cycle. **2021**, ed. by Alderton, D.; Elias, S. A., 393–398.

(2) Ward, R.; M.Robinson Principles of Hydrology - Fourth Edition. **2000**, *4*, 91–138.

(3) Zhao, L.; Xia, J.; Xu, C.-y.; Wang, Z.; Sobkowiak, L.; Long, C. Evapotranspiration estimation methods in hydrological models. *Journal of Geographical Sciences* **2013**, *23*, 359–369.

(4) Sitterson, J.; Knightes, C.; Parmar, R.; Wolfe, K.; Avant, B.; Muche, M. An overview of rainfall-runoff model types. **2018**.

(5) Oudin, L.; Hervieu, F.; Michel, C.; Perrin, C.; Andréassian, V.; Anctil, F.; Loumagne, C. Which potential evapotranspiration input for a lumped rainfall–runoff model?: Part 2—Towards a simple and efficient potential evapotranspiration model for rainfall–runoff modelling. *Journal of Hydrology* **2005**, *303*, 290–306.

(6) Bai, P.; Liu, X.; Yang, T.; Li, F.; Liang, K.; Hu, S.; Liu, C. Assessment of the Influences of Different Potential Evapotranspiration Inputs on the Performance of Monthly Hydrological Models under Different Climatic Conditions. *Journal of Hydrometeorology* **2016**, *17*, 2259–2274.

(7) Dakhlaoui, H.; Seibert, J.; Hakala, K. Sensitivity of discharge projections to potential evapotranspiration estimation in Northern Tunisia. *Regional Environmental Change* **2020**, *20*, 1–12.

(8) Ali, A.; Xiao, C.; Zhang, X.-p.; Adnan, M.; Iqbal, M.; Khan, G. Projection of future streamflow of the Hunza River Basin, Karakoram Range (Pakistan) using HBV hydrological model. *Journal of Mountain Science* **2018**, *15*, 2218–2235.

(9) Weiß, M.; Menzel, L. A global comparison of four potential evapotranspiration equations and their relevance to stream flow modelling in semi-arid environments. *Advances in Geosciences* **2008**, *18*, 15–23.

(10) Seong, C.; Sridhar, V.; Billah, M. M. Implications of potential evapotranspiration methods for streamflow estimations under changing climatic conditions. *International Journal of Climatology* **2018**, *38*, 896–914.

(11) Motavita, D.; Chow, R.; Guthke, A.; Nowak, W. The comprehensive differential split-sample test: A stress-test for hydrological model robustness under climate variability. *Journal of Hydrology* **2019**, *573*, 501–515.

(12) Dakhlaoui, H.; Ruelland, D.; Tramblay, Y.; Bargaoui, Z. Evaluating the robustness of conceptual rainfall-runoff models under climate variability in northern Tunisia. *Journal of Hydrology* **2017**, *550*, 201–217.

(13) Seibert, J. Reliability of Model Predictions Outside Calibration Conditions: Paper presented at the Nordic Hydrological Conference (Røros, Norway 4-7 August 2002). *Hydrology Research* **2003**, *34*, 477–492.

(14) Dakhlaoui, H.; Ruelland, D.; Tramblay, Y. A bootstrap-based differential split-sample test to assess the transferability of conceptual rainfall-runoff models under past and future climate variability. *Journal of Hydrology* **2019**, *575*, 470–486.

(15) Pascual Ferrer, J.; Candela Lledó, L. Water balance on the Central Rift Valley. **2015**.

(16) Hargreaves, G. H.; Samani, Z. A. Reference crop evapotranspiration from temperature. *Applied engineering in agriculture* **1985**, *1*, 96–99.

(17) Allan, R.; Pereira, L. Crop evapotranspiration-Guidelines for computing crop water requirements-FAO Irrigation and drainage paper 56. **1998**, *56*.

(18) Shirmohammadi-Aliakbarkhani, Z.; Saberali, S. F. Evaluating of eight evapotranspiration estimation methods in arid regions of Iran. *Agricultural Water Management* **2020**, *239*, 106243.

(19) Weather; climate Average monthly rainfall, temperature and sunshine Östersund.

(20) Bergström, S. Development and Application of a Conceptual Runoff Model for Scandinavian Catchments. *SMHI Rep. RHO 7* **1976**, *134 pp.*

(21) Knoben, W. J.; Freer, J. E.; Woods, R. A. Inherent benchmark or not? Comparing Nash–Sutcliffe and Kling–Gupta efficiency scores. *Hydrology and Earth System Sciences* **2019**, *23*, 4323–4331.

(22) Smith, A.; Freer, J.; Bates, P.; Sampson, C. Comparing ensemble projections of flooding against flood estimation by continuous simulation. *Journal of Hydrology* **2014**, *511*, 205–219.

(23) Jillo, A.; Demissie, S.; Viglione, A.; Asfaw, D.; Sivapalan, M. Characterization of regional variability of seasonal water balance within Omo-Ghibe River Basin, Ethiopia. *Hydrological Sciences Journal* **2017**, *62*, DOI: `10.1080/02626667.2017.1313419`.

(24) SMHI Årlig potentiell avdunstning medelvärde 1961-1990.